Technische Universität Hamburg

Institute of Environmental Technology and Energy Economics

Master's thesis

Model of the thermal behaviour of a borehole heat exchanger as a part of a hybrid energy system.

Conrado García Salinas

Matriculation number: 53576

Study programme: Erasmus

First examiner: Martin Kaltschmitt

Second examiner: Daniel Christ

Hamburg, 23/06/2020

Statutory Declaration

I hereby declare that I have authored this thesis independently, that I have not used other than the declared sources / resources, and that I have explicitly marked all material which has been quoted either literally or by content from the used sources.

Hamburg, 23/06/2020

Conrado García Salinas

Preamble

This master's thesis was executed at the Institute of Environmental Technology and Energy Economics at Technische Universität Hamburg.

Hamburg, 23/06/2020

Conrado García Salinas

Table of contents

Glossary

Roman letters

A	Coefficient matrix of the system	
a	Thermal diffusivity	m^2/s
b	Vector of independent terms	
C	Volume heat capacity	J/K
Cp	Specific heat capacity	$\dfrac{J}{kg*K}$
cpf	Specific heat capacity of the fluid	$\dfrac{J}{m^3*K}$
D	Nominal diameter of the pipe	m
h	Convection heat transfer coefficient	$\dfrac{w}{m^2*K}$
I	Intensity of current	A
i	Discretization in the radial direction	
j	Discretization in the vertical direction	
L	Length of the borehole	m
m	Volumetric flow rate	kg/s
Nu	Nusselt's Number	
Pr	Prandtl's Number	
Q	Heat flow	J
q	Heat flow per unit of length	J/m
r	radius	m
rm	Centroid of the annular region	m
rmax	Maximum radius from the axis of the borehole to undisturbed ground temperature	m
R	Thermal resistance in the radial direction	W/m
Re	Reynold's number	
Rpp	Thermal resistance between pipes	W/m
R'	Thermal resistance in the vertical direction	W/m
T	Temperature	K
Tsurface	Temperature of the surface layer	K
Tm	Undisturbed ground temperature	K
V	Voltage	V
Vf	Speed of the fluid	m/s

Greek letters

λ	Thermal conductivity	W/m
ρ	Density	$\frac{kg}{m3}$
τ	timestep	s
$\Delta\tau$	Discreitzation of time	
Δz	Increment in vertical dimension	
δr	Gap between duct and soil	m
π	Number pi	

Indices

subindices:

b	borehole
fc	convection
g	grout
p	pipe
s	soil
c	contact

Abbreviations

BHE	Borehole Heat Exchanger
GSHP	Ground Source Heat Pump

List of figures

List of tables

1 Introduction, Scope and Motivation

1.1 Introduction

Ground Heat Source Pumps (GHSP) are generally considered as highly efficient technologies that enables buildings and installations to increase energy efficiency by taking advantage of the big thermal capacity of soil in order to cool or heat a fluid. This fluid can be used later in a variety of applications. For example, in the case of house control temperature, a GHSP will use during summer the temperature of the ground, which is lower than that of the air, to cool down a fluid which is used later in radiators. I winter, on the other hande, the temperature of the ground is higher, than that of the air, so the system heats up the building.

The big thermal capacity of soil also allows to keep some heat within for long periods, this energy stored in the soil can later be used for different applications. Therefore, there is a need to understand how heat transfer processes take place in the soil. This knowledge can eventually lead to an improvement in GHSP design and further adapted usage.

GHSP and their interaction with soil temperature have been extensively studied. One of the main sources of information is provided by (Hellström, 1991), who develops a complete theory of heat transfer in boreholes.

(Zarrella, De Carli, Tonon, & Zecchini, 2009) presents a computational model (CaRM model), that takes advantage of the electrical approach to discretize and model both soil and GHSP. This solution provides flexibility and accuracy to simulate the thermal behavior of the GHSP under different circumstances.

The main goal of this study is to implement the model proposed in (Zarrella, De Carli, Tonon, & Zecchini, 2009) for Single U-pipe heat exchanger in a Matlab script, in order to build a tool that enables to conduct different simulations and explore the influence of different parameters. More importantly, this tool would be able to interact with other scripts, so other researchers can use it for their investigations.

1.2 Aims and Scope

The main goals of this thesis are listed below:

- Development of a model which describes the heat transfer in the soil and it most relevant properties.
- Investigation of the effect of long-term seasonal heat injection into the soil.
- Quantification of heat injected and extracted in the soil during a certain period.
- Sensitivity analysis of different variables of the model in order to observe their influence.

The format of the model should be a Matlab file intended to interact with other models developed within the "HySol" project in the Institut für Umwelttechnik und Energiewirtwschaft, which is part of the Hamburg University of Technology (TUHH).

This study is structured in 8 chapters; After Introduction of chapter one, a brief theoretical background is developed in chapter 2. This review of existing knowledge covers both borehole heat exchangers (BHE) and soil modelling. chapter 3 covers how the model is built by means of the equivalence between electric and thermal modelling. Assumptions, simplifications and equations used in the developed model are also detailed here. In chapter 4 the influence of the mesh size used in the modelling is discussed. Chapter 5 present the cases that have been simulated and chapter 6 shows the results of the cases introduced in chapter 5. Chapter 7 and 8 are the conclusions of the study and the references used respectively.

2   Theoretical Background

A review of the technology that is used for the development of the model is carried out in this section. First of all, a full description of the main characteristics of BHEs and mathematical modelling is provided. Then, the main characteristics of soil and the effect of different variables in these characteristics, such as water content or temperature, are described.

2.1   Types of borehole heat exchanger BHE

Regarding energy efficiency in buildings, the most common kinds of BHE are the single U, double U and concentric boreholes. The working principle is the same for all of them. A fluid circulates within a pipe, which is inserted into a grout, the differences of temperature between the fluid and the surrounding grout creating therefore a heat flow..

Single U

The single U type of a BHE has one pipe for containing the fluid while at the bottom of the borehole, this very same pipe returns upwards. Generally, the notation of 2 pipes is used. This is the simplest configuration and the one of which this study is based.

Double U

Is the same concept that with single U, but having two loops instead of one. In addition, there are two types of connection for these U pipes. If the end of one loop is connected to the beginning of the other, it is said that they are connected in series. On the other hand, if they work as two independent single U pipes they are in parallel.

Concentric

The input pipe is placed inside another pipe that will provide the output. The fluid scapes at the bottom of the borehole and returns surrounding the inner pipe.

In fig 1 (Silwa, 2015) these three kinds of BHE can be observed. (a) Represents a single U borehole. (b) represents a double U borehole and (c) represents a concentric BHE.
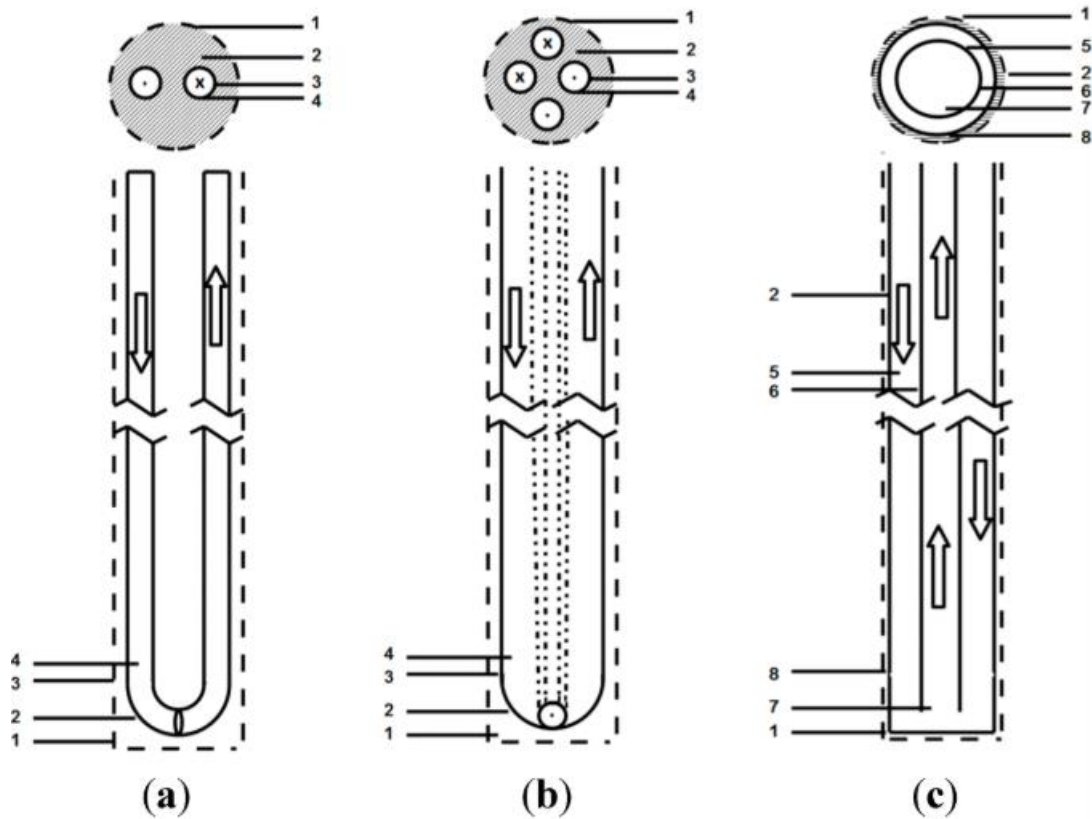
Figure 1 Single U (a) Double U (b) and concentric (c)

2.2 Heat conduction in boreholes

Heat transfer from fluid to soil is described below. There are two ways of heat transferring in a BHE: Convection between the fluid and the pipe and conduction between the pipe wall and the BHE`s wall. The amount of heat transferred, and temperatures of both the fluid and wall of the BHE depends of the different materials, flow rate, and geometry of the BHE.

Convection

In (Hellström, 1991) a complete description of this phenomenon for the case of BHE is found.

In general, heat transfer by convection can be assessed by means of Nusselt`s number which is defined in Eq 1:

$$Nu = \frac{Actual\ Heat\ transfer}{Conductive\ Heat\ transfer} \qquad \text{Eq 1}$$

The expressions of Nu depend of Reynolds number, that for the case of circular pipe takes the shape shown in Eq 2.

$$Re = \frac{v_f * \rho_f * 2 * r_p}{\mu_f} \qquad \text{Eq 2}$$

Where v_f is the velocity of the fluid, ρ_f is the density of the fluid, r_p is the radius of the pipe and μ_f is the dynamic viscosity of the fluid.

Depending on the values of Re, the fluid regime is considered to be a full laminar flow if Re <2300; full turbulent flow if Re >10000 or in a transition zone if the value is between 2300 and 10000.

According to the different type of flow, a certain expression for Nu is used. In the case of convection within a pipe, Prandtl`s number according with Eq 3.

$$Pr = \frac{\mu_f * c_f}{\lambda_f} \qquad \text{Eq 3}$$

Where c_f the heat capacity of the fluid, and λ_f is its thermal conductivity.

The expressions for Nusselt´s number are obtained from Eq4 and Eq5 (Schlünder, 1983). The last expression Eq 6 is the correlation from Dittus-Boelter (Dittus FW, 1930.)

$$Nu = 1.16 * \left(Re * Pr * \frac{D}{L} \right)^{\frac{1}{3}} \qquad (Re < 2000) \qquad \text{Eq 4}$$

$$Nu = 0.116 * \left(Re^{\frac{2}{3}} - 1.25 \right) * Pr^{\frac{1}{3}} * \left(1 + \frac{D}{L} \right)^{\frac{2}{3}} \qquad (2000 < Re < 10000) \qquad \text{Eq 5}$$

$$Nu = 0.023 * Re^{0.8} * Pr^{0.4} \qquad (Re > 10000) \qquad heating \qquad \text{Eq 6}$$
$$Nu = 0.023 * Re^{0.8} * Pr^{0.3} \qquad (Re > 10000) \qquad cooling$$

In these expressions D is the inner diameter and L is the length of the pipe on study. For single U pipes, double U pipes and concentric BHE`s, this value is equal to the depth of the borehole.

Once Nusselt`s number is calculated, the coefficient of heat transfer h is derived from Eq 7:

$$Nu = \frac{q'actual}{q'cond} = h * \frac{L}{\lambda_f} \qquad \text{Eq 7}$$

Conduction

From the pipe to the ground, heat transfer takes place just by conduction (Hellström, 1991). It is common to assess the problem of heat transferring by means of the thermoelectrical equivalence in cylindrical coordinates (D. Bauer, 2010).

There is an equivalence between thermodynamics and electricity, so it is possible to use the same approach.

To sum up, the heat transfer between two points can be written, as it is found in Eq 8 (Hellström, 1991):

$$T1 - T2 = R * q \qquad \text{Eq 8}$$

Which is the equivalent of the Ohm`s law expression as shown in Eq 9:

$$V1 - V2 = R * I \qquad \text{Eq 9}$$

Where V stands for voltage, I refers to intensity of current and R means electrical resistance. Therefore, temperatures are equivalent to voltages, intensity to heat flux and the relation among them, resistances.

This is also the case of BHE`s, that according to (Hellström, 1991) can be described as follows for a single U BHE (shown in fig 2) (Hellström, 1991):
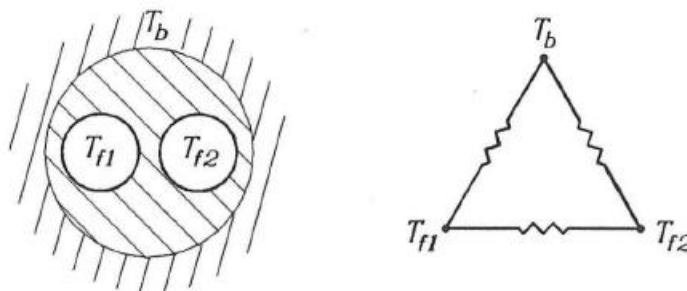

Figure 2 Electric model of a Single U BHE

Here Tf1 and Tf2 correlates to the temperature of the inlet and outlet fluid, whereas Tb is the temperature of the borehole wall.

The calculation of the resistances between the pipe and the borehole wall as well as between the pipes is detailed in (Hellström, 1991) (D. Bauer, 2010) and specially in (Al-Chalabi, 2013) where different approaches are summarized.

The resistance between the fluid and the borehole, R_b, accounts for three processes: convection between fluid and pipe, conduction through the pipe and conduction through grout. According to (Al-Chalabi, 2013) processes can be presented as shown in Eq 10:

$$R_b = Rfc + Rp + R_g \qquad \text{Eq 10}$$

Where R_f is the convective resistance between fluid and pipe, R_p is the resistance in the pipe and R_g is the resistance of the grout.

R_f is obtained by means of the previously defined Nusselt`s number (Eq 7) following the expression:

$$R_{fc} = \frac{1}{2 * \pi * h * r_1} \qquad \text{Eq 11}$$

Where h is the convective heat transfer factor, analogue to α of eq 7, and r_1 is equal to the inner radius of the pipe.

The resistance of the pipe follows Eq 12 (Incropera, 2007)

$$R_p = \frac{\ln\left(\frac{r_2}{r_1}\right)}{2 * \pi * \lambda} \qquad \text{Eq 12}$$

Where r_1 is the inner radius of the pipe, r_2 the outer radius of the pipe, and λ the thermal conductivity of the pipe material.

If the material surrounding the pipes is soil, then (Hellström, 1991) proposes the addition of a contact resistance, shown in Eq 13:

$$R_c = \frac{1 * \delta r}{2 * \pi * \lambda * r_2} \qquad \text{Eq 13}$$

Where δr is the thin gap between pipe and soil, in case it exists and is small compared with r_2.

However, several studies have been carried out in order to estimate a suitable value of R_b. In (Al-Chalabi, 2013) a comparative among the models proposed by (Intemann, 1982), (Gu, 1998), (Hellström, 1991), (Bennet, 1987), (Shonder, 1999), and (Sharqawy, 2009) is found.

The main conclusion is that Eq 14 which is provided by (Bennet, 1987) is the one that gives the most accurate estimation of R_b

$$R_b = \frac{1}{4 * \pi * \lambda_g} * \left[\ln\left(\frac{\lambda_1 \lambda_2^{1+4\sigma}}{2 * (\lambda_2^4 - 1)^\sigma} \right) - \frac{\lambda_3^2 (1 - \left(\frac{4\sigma}{\lambda_2^4} - 1\right)))^\wedge 2}{1 + \lambda_3^2 (1 + \frac{16\sigma}{(\lambda_2^2 - (\frac{1}{\lambda_2^2}))^\wedge 2})} \right]$$

Eq 14

Where $\lambda_1 = \frac{rb}{rp}, \lambda_2 = \frac{db}{s}, \lambda_3 = \frac{\lambda_2}{2*\lambda_1}, \sigma = \frac{\lambda_g - \lambda_s}{\lambda_g + \lambda_s}$ with rb being the borehole radius (m), rp is the pipe radius, λ_g is the grout thermal conductivity (W/K*m) and λ_s is the soil thermal conductivity (W/K*m).

Therefore, the temperature in the borehole wall can be obtained from the inlet and outlet temperature just by performing an energy balance, as presented in Eq 15. This balance neglects the temperature change within the borehole.

$$\frac{T_{f1} - T_b}{R_b} + \frac{T_{f2} - T_b}{R_b} = 0$$

Eq 15

2.3 Soil modelling

A review of the most important characteristics of the soil is presented in this section. First a brief resume of the kinds of soil and the physical properties that influences its thermal response is presented. After that, the model developed by Kersten is shown. Finally, the approach that has been used in this paper is presented.

2.3.1 Characteristics

The most important parameters that influences thermal response are thermal conductivity, λ $(\frac{K}{W*m})$, heat capacity Cp $\left(\frac{J}{Kg*K}\right)$ and soil density ρ $(\frac{kg}{m^3})$. Together they give place to thermal diffusivity a $(\frac{m^2}{s})$, which is the ratio of heat is conductivity through soil as shown in Eq 16:

$$a = \frac{\lambda}{Cp * \rho} \qquad\qquad \text{Eq 16}$$

Typical values of thermal diffusivity are 0.005×10^4 - 0.02×10^4, as cited in (Al-Chalabi, 2013)

As appears in (Kersten, 1949), thermal conductivity, heat capacity and soil density are intimately ligated to the structure of the soil. Soil is made of three phases, solid, water and air, whose proportions, the so-called volumetric fraction, influences these variables. In table 1 some values of thermal conductivity are shown (Al-Chalabi, 2013)

Thermal conductivity is especially sensitive to the influence of water phase, which is called soil moisture. An increment of soil moisture leads to a rise of conductivity. Another parameter that influences thermal conductivity is dry density, that accounts for the particles of soil per unit of volume. If dry density increases, so does the thermal conductivity. Thermal conductivity of different types of soil depending on their soil moisture can be found in fig 3 (Kersten, 1949).

Table 1 Thermal conductivity of most common soils

Class	Thermal Conductivity W m-1K-1
Gravel	0.77
Silt	1.67
Clay	1.11
Loam	0.91
Saturated sand	2.5
Saturated silt or clay	1.67
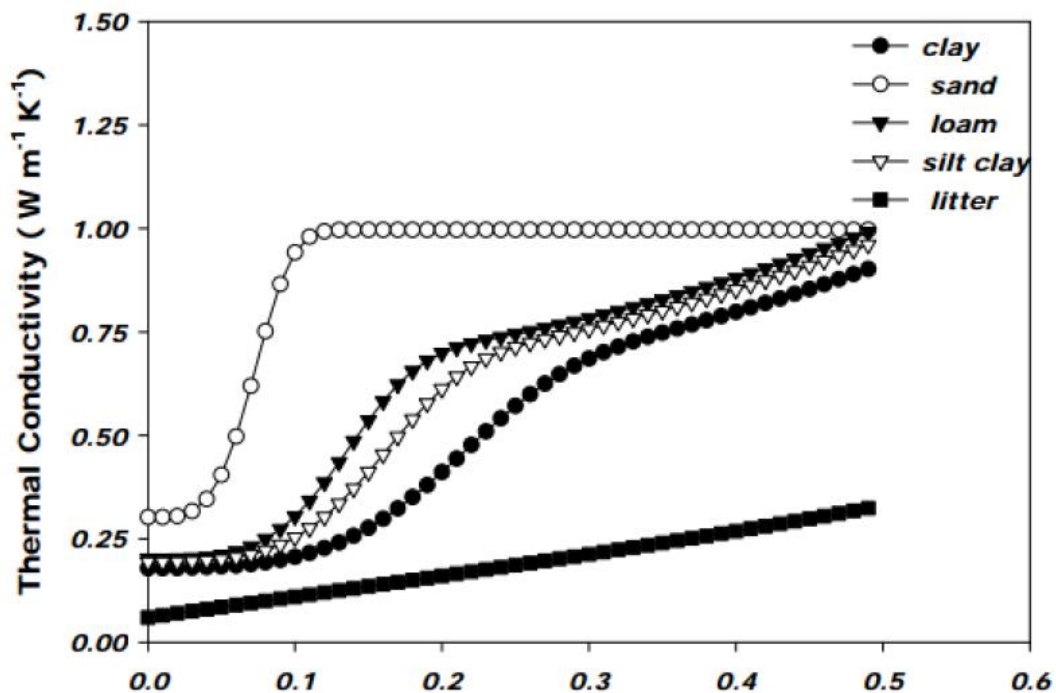
Figure 3 Influence of soil moisture in thermal conductivity

As shown in fig 3, the increment of thermal conductivity with soil moisture is in general not linear with the exception of litter. The reason for this increment is that water replaces air in the pores of the different soils and, since water has a higher thermal conductivity than air, the overall thermal conductivity increases. Porous materials such as sand, are more prone to suffer this effect.

Heat capacity is also crucial, as this parameter account for the amount of heat which can be extracted from every degree of variance in the soil. If a substance has a great heat capacity, a lot of heat can be extracted or injected with a small change in its temperature which is the case of most soils.

Heat capacity is also influenced by soil moisture, because heat capacity of the soil is just the sum of the different heat capacities of its components and water has a relatively big Cp (4.18 MJ/m^3) (Kersten, 1949).

Since soil moisture affects both thermal conductivity and heat capacity, it is worthy to ask if this parameter is constant over time. Soil moisture depends on the fluxes of water through the soil, and it is influenced by weather in the upper layers of soil. Later, this water will go downwards to the inner layers. However, regarding the study of big BHE`s, with hundreds of meters of depth, this parameter is usually considered as constant (Hellström, 1991).

Another parameter that may affect both conductivity and capacity is temperature. Typically, an undisturbed ground temperature is considered, however with operation time, this temperature will change, and this change can affect conductivity and capacity.

(Kersten, 1949) concluded a 4% decrease in resistivity for a 17°C increase in temperature and about a 10 % decrease in resistivity for an increase in temperature in the range of 20°C to 60°C.

2.3.2   Estimation of soil conductivity

Wide research have been conducted on this field as found in (Kersten, 1949), (Tarnawski, 2000) and (Johansen, 1977) .

The analytical formula that takes the geometric mean approach is found in (Kersten, 1949) and presented in Eq 17.

$$\lambda_T = \lambda_s^{1-n} * \lambda_w^n$$ Eq 17

Where λ_T is the thermal conductivity of soil, λ_s is the thermal conductivity of the solid fraction and λ_w is the thermal conductivity of the water fraction. n is the soil porosity.

(Al-Chalabi, 2013) brings up the fact that this equation is valid only if the conductivities of the different components do not contrast more than one order of magnitude. Other researches such as (De Vries D. , 2002) and (Silva, 1985) present empirical equations that are valid only under certain conditions. In this study, the value of thermal conductivity for different soils has been obtained from other papers and databases.

3 Materials and Methods

In this section, the general model of borehole and soil are put together and the main assumptions and simplifications are discussed. Verification is also carried out.

3.1 Electric circuit

In order to describe the heat fluxes in the soil, the approach of the Ladder equivalent electric circuit is taken from (Zarrella, De Carli, Tonon, & Zecchini, 2009).

In this approach a cylindrical portion of soil has a thermal resistance, which depends on thermal conductivity and its thickness plus a thermal capacitance, which depends on the thermal capacity. Studies of the temperature of the soil using this model have been conducted in (Zarrella, De Carli, Tonon, & Zecchini, 2009) and (M. Diaz-Aguiló, 2014)

Therefore, it is possible to describe a cylindrical control volume in which centre is located the BHE. This cylinder can be discretised into several concentric annular regions and layers of depth. This is which (in advance) will be referred to as "mesh". Fig 4 (Zarrella, De Carli, Tonon, & Zecchini, 2009) illustrates the method.
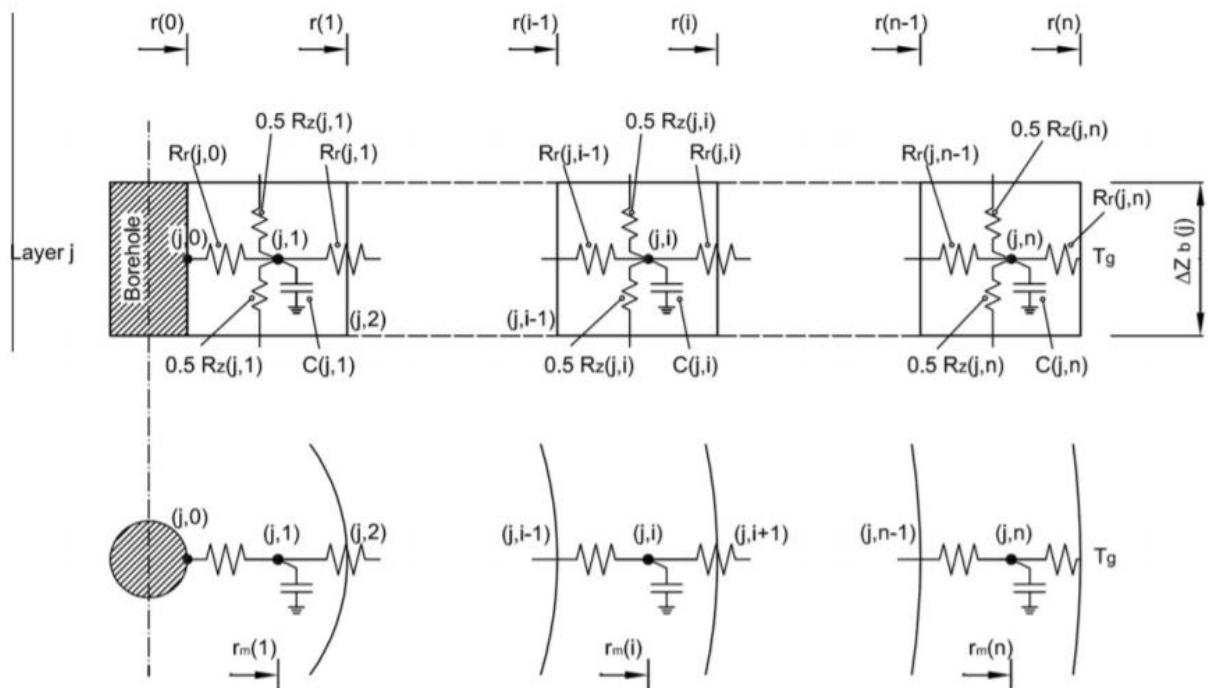

Figure 4 Soil discretization and modelling

The cylinder of radius equal to *rmax* is divided into i-annular regions and j-layers of depth. Then, according to (Zarrella, De Carli, Tonon, & Zecchini, 2009) each annulus will be defined by means of a thermal resistance and a thermal capacity as shown in Eq 18:

$$R(i,j) = \frac{1}{\lambda * 2 * \pi} * \ln(\frac{rm(i)}{rm(i-1)})$$

Eq 18

Where $R(i,j)$ is the thermal resistance of the I annular region at a j layer of depth, λ (K/W) is the thermal conductivity of the soil, i is the *i*-annular region, j is the *j*-layer of depth and *rm* is the centroid of the annular region (m) which is given by Eq19 (Zarrella, De Carli, Tonon, & Zecchini, 2009).

$$rm(i) = \sqrt{\frac{r(i)^2 + r(i-1)^2}{2}}$$

Eq 19

At this point *rm(i)* the thermal capacity is lumped, and has the shape given by Eq 20 (Zarrella, De Carli, Tonon, & Zecchini, 2009).

$$C(i,j) = Cp(i,j) * \rho * V(i,j) = Cp(i,j) * \rho * \pi * (r(i)^2 - r(i-1)^2 * \Delta z$$

Eq 20

Where $Cp(i,j)$ is the thermal capacity of the soil (J/kg*K), ρ is the density of the soil (kg/m3) and Δz is the depth of each layer.

The vertical resistance, $Rz(j)$ is given by Eq 21 (Zarrella, De Carli, Tonon, & Zecchini, 2009)

$$Rz(j) = \frac{\Delta z}{\lambda} * \frac{1}{\pi * (r^2(i) - r^2(i-1))}$$

Eq 21

Where Δz is the thickness of every layer in the vertical direction.

3.2 General equivalent circuit

In previous section 2.2, the modelling of the borehole has been discussed. This model describes the heat flux from the pipes to borehole wall. Later, on section **Error! Reference source not found.** the modelling of the surrounding soil was carried out. This model starts in the borehole wall and finishes in a point of the soil at a certain radius distance *rmax*. By putting altogether, a model that describes the heat flux from the fluid temperature to certain point in the ground is achieved as shown in fig 5 (Zarrella, De Carli, Tonon, & Zecchini, 2009).
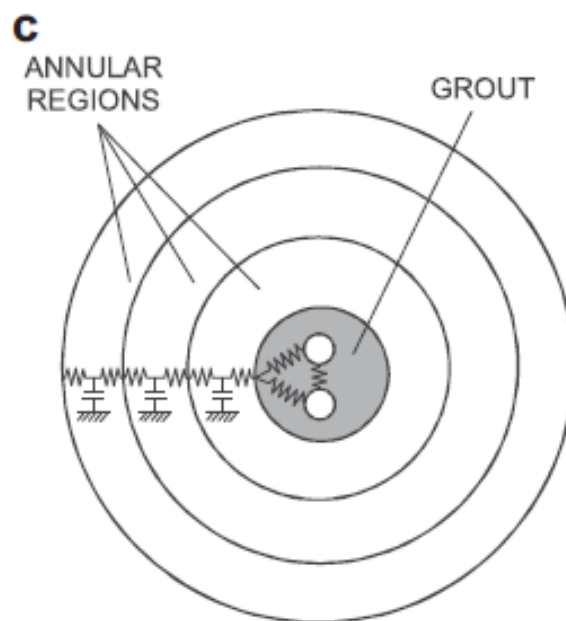

Figure 5 Borehole and soil models

3.3 Influence of surface temperature

In most of the reviewed literature the assumption of no heat transfer between the different *j* layers is accepted, and (Hellström, 1991) and (Zarrella, De Carli, Tonon, & Zecchini, 2009) state that for deep boreholes, the effect of the surface temperature is to be neglected, because it is only important in the upper layers. However, the case of study in this thesis has only 15 m depth, so the axial heat transfer must be considered.

Other investigations such as (Fürtbauer, 2019) (Alam, 2015) or (Evans, 2010) quantify this effect. (Evans, 2010) provides the following graph (fig 6).
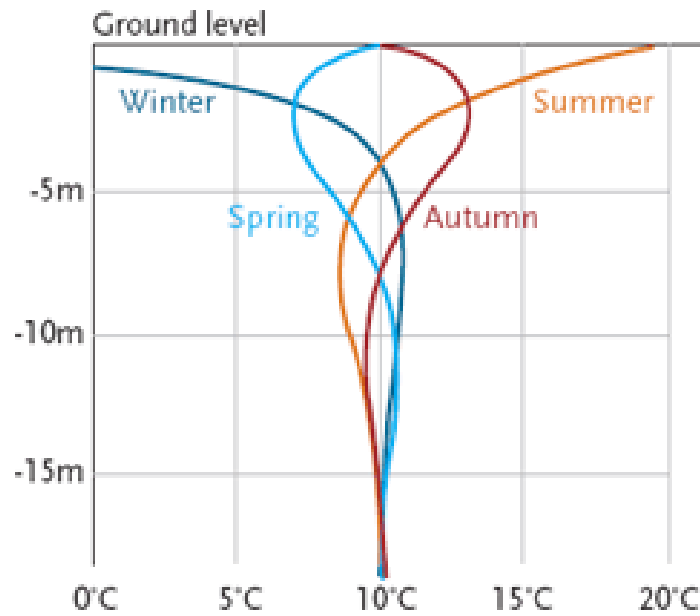
Figure 6 Evolution of soil temperature with depth

As can be seen in figure 6, there is a trend to establish with depth around a certain value that depends on the location of the study. For Germany this steady value is usually considered to be 283 K (Evans, 2010)

3.4 Assumption and simplifications

In order to simulate the model, some assumptions have been taken for reducing its complexity

Temperature of the ground surface

The temperature of the ground surface represents a challenge, due to the fact that it depends on the vegetal coverage, the kind of soil, the irradiation, the air temperature, the speed of the wind among other factors. There is no analytical solution yet for this problem and it is a variable that can vary a lot. So, the approach given in this thesis relies on taking the air temperature and artificially decrease its variation, because ground surface temperature must vary with this temperature, but to a lesser extent.

The temperature of the ground surface is computed as follows from Eq 22:

$$Tsurface(t) = 283 + \frac{Tair(t) - average}{4} \qquad \text{Eq 22}$$

The average value is the yearly average of the temperature of the air and in the dataset used in this study has a value of 10.257.
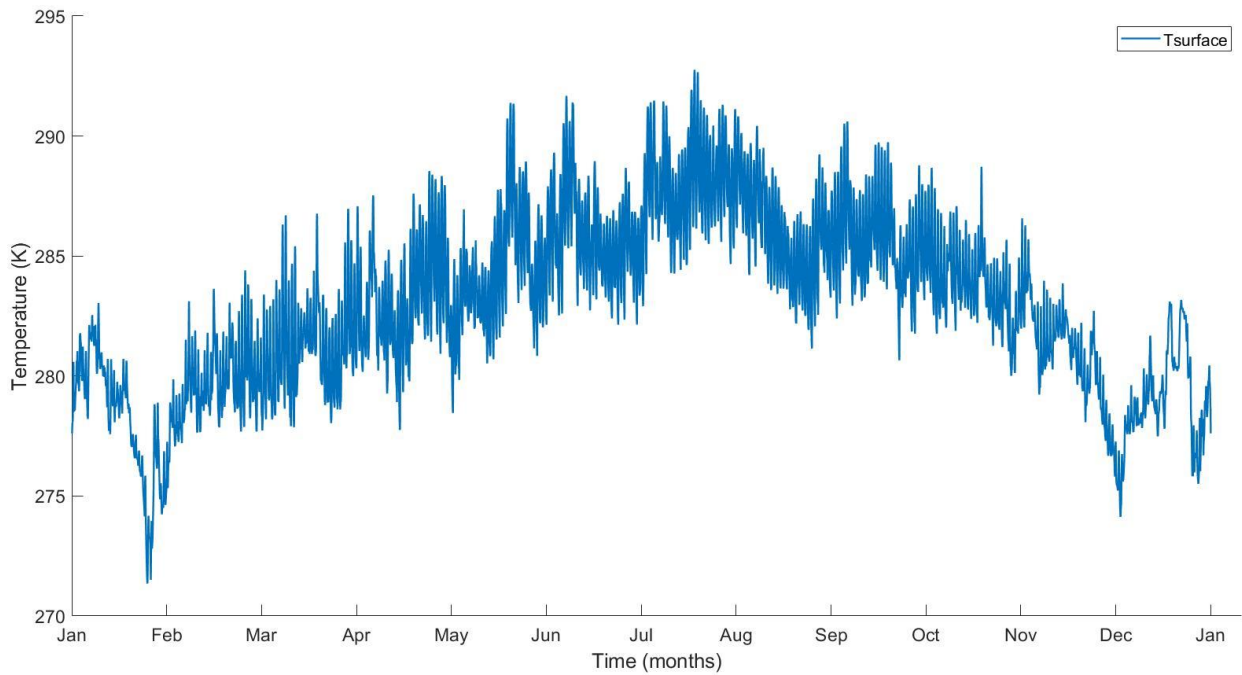

Figure 7 Temperature of surface in a single year

By using the previously explained technique, we have a variation in the range of approximately +- 7 K from 283K. This is easy to change by adjusting the factor of the denominator in order to get a bigger influence of the temperature of the air.

Boundary conditions

In order to simulate the model, some boundary conditions are required. First, the undisturbed ground temperature is set in the points at distance equal to *rmax*. This is because the heat flux is inexistent, since all the energy should be stored in the capacitances. The value of *rmax* is then important, as a small value could lead to miscalculations if the real temperature at *rmax* is not close enough to this undisturbed temperature. In this study 0.1 K has been considered as a difference small enough not to affect the results. If the value of *rmax* is too big, our calculations steps are being incremented with no useful data, which can lead to a big calculation time.

In the bottom of the borehole, which sets at 21 meters, the effect of the surface is negligible, according with (Evans, 2010) (Fürtbauer, 2019) (Alam, 2015), so the temperature in the 22th layer is set to 283 K as well.

3.5 System of equations

The circuit presented in section 3.2 mathematically represents a set of linear equations as presented in (Zarrella, De Carli, Tonon, & Zecchini, 2009). For every layer J, the energy balance in the different points is considered.

For every *j-th* layer, the energy balance in both pipes is calculated. In this model, the capacitance of the fluid and the pipe are neglected as shown in Eq 23.

$$\dot{m} * cpf * (Tw(j-1) - Tw(j) - 2 * \pi * rp * h * \Delta z * \left(\overline{Tw(j)} - Tp(j)\right) = 0 \quad \text{Eq 23}$$

Where $\dot{m}$ is the mass flow rate in kg/s, cpf is the fluid thermal capacity in $\frac{J}{kg*K}$ $Tw(j)$ is the temperature of the fluid leaving the layer j, $Tw1(j-1)$ is the temperature of the fluid entering the j-th layer, rp is the radius of the piep, h is the convection coefficient, Δz is the thickness of layer j-th layer, $\overline{Tw(j)}$ is the average temperature in the j-th layer that according with (Zarrella, De Carli, Tonon, & Zecchini, 2009) can be taken equal to $Tw(j)$ with acceptable error. Finally, $Tp(j)$ is the temperature of the pipe wall. Note that the term $2 * \pi * rp * h$ is equal to $\frac{1}{Rfc}$ as calculated in section 2.2 Eq 11. In fig 8 a description of the electric equivalent model for pipe 1 is given.
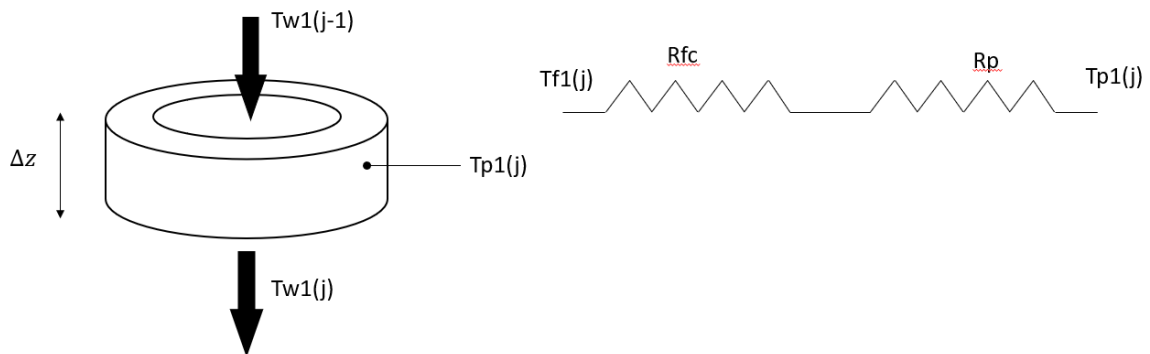

Figure 8 Heat transfer in pipe 1

Therefore, the heat balance equation for every pipe and borehole wall can be written as shown in Eq 24 and Eq 25

$$\frac{Tw1(j) - Tp1(j)}{Rfc} + \frac{Tp1(j) - Tp2(j)}{Rpp} + \frac{Tb(j) - T(j,1)}{R(j,1)} = 0 \qquad \text{Eq 24}$$

$$\frac{Tw2(j) - Tp2(j)}{Rfc} + \frac{Tp1(j) - Tp2(j)}{Rpp} + \frac{Tb(j) - T(j,1)}{R(j,1)} = 0 \qquad \text{Eq 25}$$

Where the index 1 accounts for the inlet and 2 for the outlet. Rpp is equal to the resistance between pipes and its value is calculated by means of Eq 26. $R(j,1)$ is the ground resistance of the first annular region.

$$Rpp = \frac{s - 2 * rp}{\lambda b} \qquad \text{Eq 26}$$

Where s is the space between the center of every pipe, rp is the mean radius of the pipe and λb is the thermal conductivity of the borehole material.

For the borehole wall the heat balance takes the shape:

$$\frac{Tp1(j) - Tb(j)}{Rg} + \frac{Tp2(j) - Tb(j)}{Rg} + \frac{T(1,j) - Tb(j)}{R(1,j)} = 0 \qquad \text{Eq 27}$$

Where Rg is the resistance between the pipe and the borehole wall. This value has been obtained by subtracting $Rf0$ and Rp0 from Rb as presented in Eq 10. The balance is summarized in fig 9.
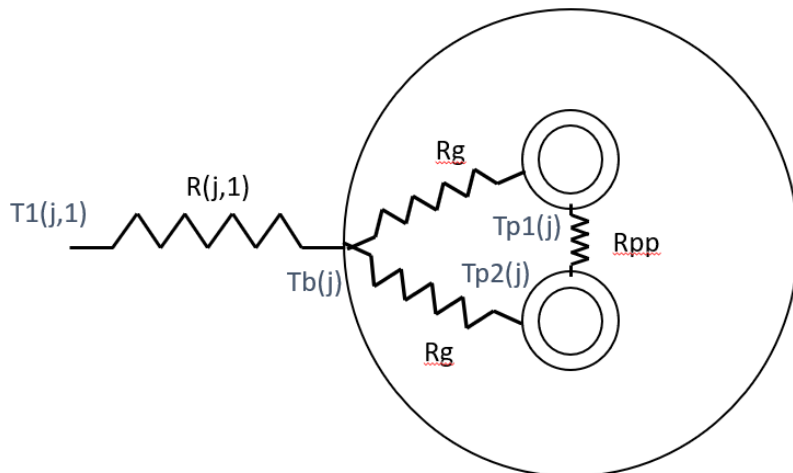

Figure 9 Detail of electric circuit of the BHE

Finally, for every annular region the energy balance takes the shape given by Eq 29

$$\frac{T(j,i-1)-T(j,i)}{R(j,i-1)} + \frac{T(j,i+1)-Tj(j,i)}{R(j,i)} + \frac{T(j-1,i)-T(j,i)}{Rz(j)}$$
$$+ \frac{T(j+1,i)-T(j,i)}{Rz(j)} = \frac{C(j,i)}{\Delta z} * T(j,i) - T(j,i)_{\Delta t}$$

Eq 29

Boundary points

$T(j,i)_{\Delta t}$ stands for the Temperature at point (j,i) in the previous step of calculation. This means, an initial temperature must be set which would be the undisturbed ground temperature *Tm=283 K.* For the points placed at the boundary of the control volume, Eq 30-32 are used.

When considering the points at a depth equal to the length of the borehole, Eq 33 gives the relation between the inlet pipe and the outlet pipe.

$$if\ i = 0 \rightarrow T(j, i-1) = Tb$$

Eq 30

$$if\ j = 0 \begin{cases} T(j-1, i) = Tsurface \\ Tw1(j) = Temp\_in \\ Tw2(j) = Temp\_out \end{cases}$$

Eq 31

$$if\ i = rmax \rightarrow T(j, i+1) = Tm$$

Eq 32

$$if\ j = depth \rightarrow Tw1(j) = Tw2(j+1)$$

Eq 33

Here $Temp\_in$ and $Temp\_out$ are the inlet and outlet fluid temperatures. In this case, just the inlet temperature is an input to the system. $Temp\_out$ is calculated within the model.

For every layer there are 3+2+n equations, so the final number of equations to be solved is m*(5+n), where n is the number of annular regions and m the number of vertical layers.

The system, which is linear, can be solved by means of the inverse matrix as shown in Eq 34. (Zarrella, De Carli, Tonon, & Zecchini, 2009)

$$[A][x] = [b] \rightarrow [x] = [A^{-1}][b] \qquad \text{Eq 34}$$

Being $[A]$ the matrix of coefficients of the system, $[x]$ the vector of unknown variables and $[b]$ the vector of independent terms. In the table below the inputs and outputs of the system are summarized.

Table 2 Inputs and Outputs to the system

INPUTS	OUTPUTS
Temperature in the inlet	Temperature of the borehole wall
Mass flow	Temperature at the outlet
Undisturbed ground temperature	Temperature field in the ground
Resistances: Rb,Rg,Rpp	Temperature of the pipes
Thermal conductivities: Fluid, soil, borehole	Temperature of the fluid
Densities: Fluid, soil	
Thermal capacities: Soil and fluid	
Geometry of the mesh (radius and thickness of vertical layers)	
Geometry of the borehole: radius of the pipes, length and shank spacing	

The temperature at the inlet is given for every time step, as presented in fig10
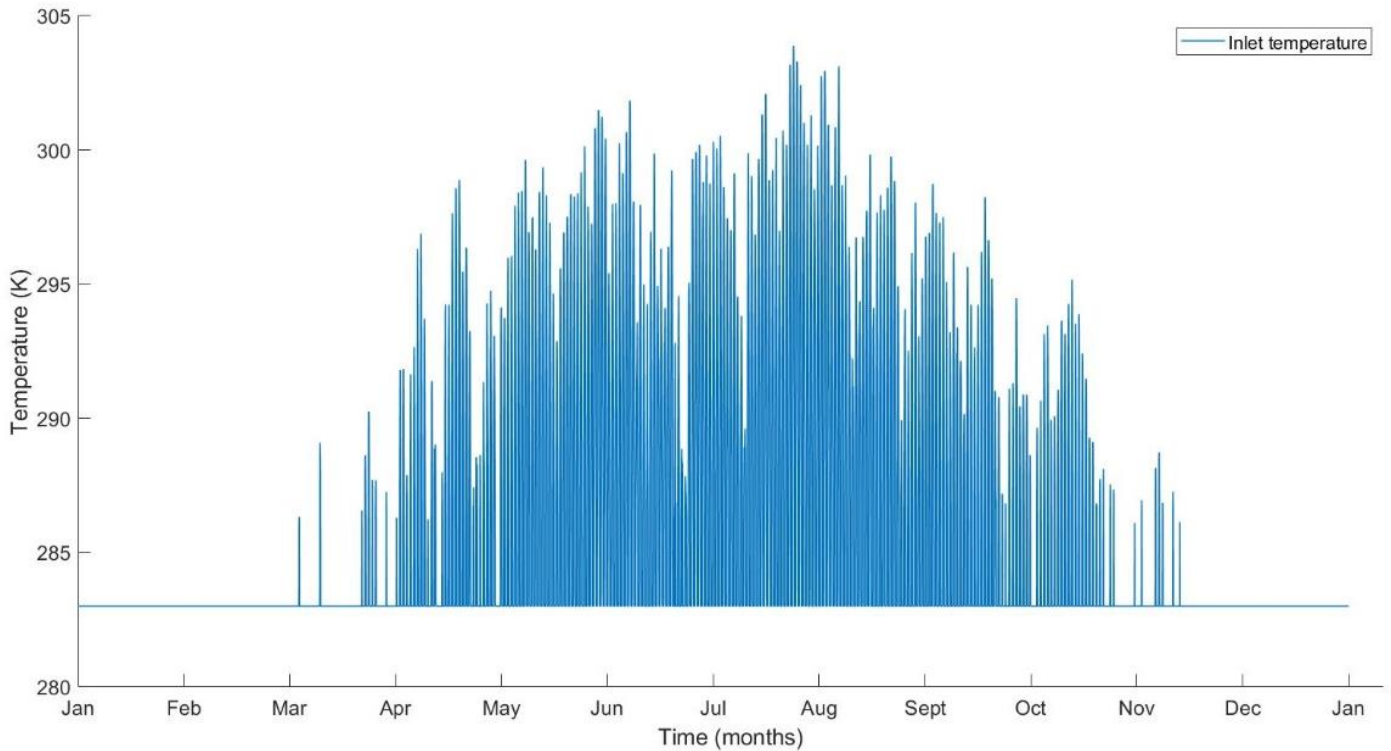

Figure 10 Inlet fluid temperature

As can be seen, the input has a base value of 283 K. In winter there is no increment of this temperature. However, in the rest of the year there is an increment with peaks up to 304 K. This behavior is due to the nature of the system that provides the data. The inlet fluid came from a photovoltaic field refrigeration system made up by a certain number of collectors. With the higher temperatures and solar radiation of spring, summer and autumn, the fluid increases its temperature and travels to the BHE in order to cool down. This is the annual input that is used in the simulations.

Finally, the amount of heat transferred is calculated by means of the well-known Eq 36 (Incropera, 2007)

$$q = \dot{m} * cpf * \Delta T \hspace{3cm} \text{Eq 36}$$

Where q is the heat transferred, $\dot{m}$ is the mass flow rate, cpf is the thermal capacity of the fluid and ΔT is the difference of temperature between he inlet and the outlet. However, this value is not equivalent to the heat stored in the ground control volume, because of the losses from the surface and the surrounding soil. The heat that is stored in the soil can be found by means of Eq37

$$qstored(t) = \sum_{j}^{H} \sum_{i}^{rmax} (T(j,i,t) - Tm) * C(j,i)$$

<div align="right">Eq 37</div>

Where *qstored* is the energy stored in the soil as increment of temperature. $T(j,i,t)$ accounts for the temperature of every region at a given time, Tm is the undisturbed ground temperature and $C(j,i)$ is the heat capacity of the region j-th,i-th. The equation expresses that the energy stored in the whole control volume for every instant of time is equal to the sum of the energy stored in the smaller regions, in which this big control volume has been discretised. This magnitude actually stands for the energy stored in the soil that has been delivered by the BHE and exchanged through the surface since it is calculated taking Tm as a reference point.

4 Effect of mesh size

When using this approach it is of interest the study of the mesh size. As stated in (M. Díaz-Aguiló, 2015), There is big gradient of temperatures in the proximities of the heat source. This means that the mesh size should be small in order to allow to extract all the information. However, in regions far away from the heat source, it is sufficient with a thick layer, as the range of temperatures are smaller and will converge to the undisturbed ground temperature.

It is important to note that sometimes is not efficient to run a simulation with a small mesh size that covers all the ground because the computation time increase dramatically with the number of mesh elements. The solution proposed by (M. Diaz-Aguiló, 2014) consists in an exponential distribution of the soil layers as illustrated in fig. 11-
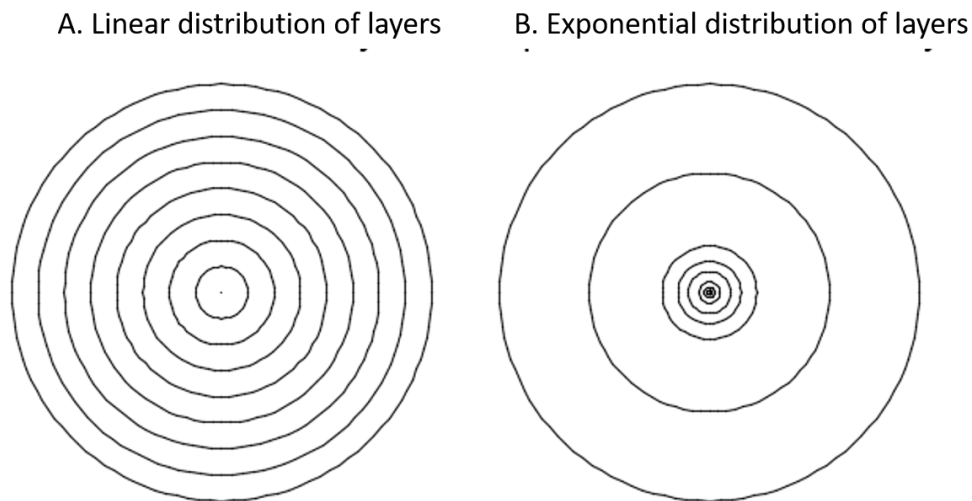
A. Linear distribution of layers   B. Exponential distribution of layers

Figure 11 Linear distributions of layers vs Exponential distribution of layers

This exponential distribution is computed by means of Eq 35, also found in (M. Díaz-Aguiló, 2015)

$$b(i) = rb - (rmax - rb) * \frac{e^{(\gamma * i)} - 1}{e^{(N)} - 1}$$

Eq 35

Where $b(i)$ us the vector with the radial boundaries of the layers, rb is the borehole radius. $rmax$ is the maximum radius considered at which distance the boundary condition of $T = Tm$ is set. N is the number of layers and γ is the exponential factor, that must be a positive value.

5   Cases of study

In this section, the different simulations conducted are presented and discussed. Basically, the different simulations consist on a base case upon a sensitivity analysis was conducted in order to investigate the effect of the kind of soil, the number of collectors and the dimension of the mesh.

5.1   Base case

The presented model has been tested in different situations in order to investigate the effect of different variables in its behavior.

The geometry of the single U heat exchanger that has been taken for study is detailed in Table 3. (Al-Chalabi, 2013)

Table 3 Geometry of the studied borehole

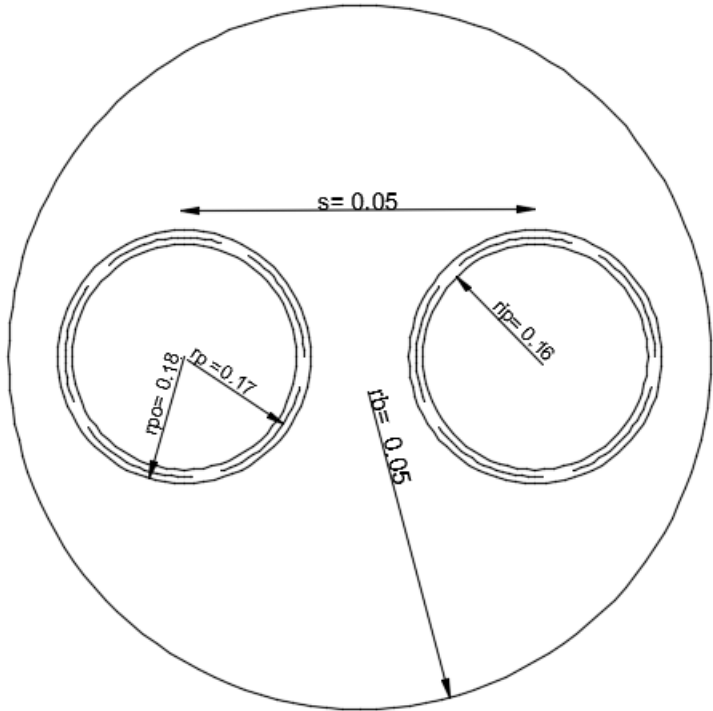| MAGNITUDE	VARIABLE	VALUE (M)
RADIUS OF THE BOREHOLE	rb	0.05
NUMBER OF PIPES	-	2
INNER RADIUS OF PIPES	rip	0.016
OUTER RADIUS OF PIPES	rop	0.018
MEAN RADIUS OF PIPES	rp	0.017
SHANK SPACING	s	0.05
LENGTH	-	21

Figure 12 Geometry of the borehole

For the base case, which is the one that serves as reference in this study, the different parameters of the simulation are summarized in Table 4.

Table 4 Parameters of the simulation-General case

Magnitude	Value	Units
Thermal conductivity of the pipe	17	W/m
Thermal conductivity of the borehole	0.77	W/m
Thermal conductivity of the fluid	0.5918	W/m
Thermal conductivity of the soil	0.77	W/m
Thermal capacity of the soil	1000	J/kg*K
Thermal capacity of the fluid	41800000	J/kg*K
Density of the soil	2000	Kg/m^3
Density of the fluid	1000	Kg/m^3
Viscosity of the fluid	0.001	N/s*m^2
Undisturbed ground temperature	283	K
Number of collectors	16	
Mass flow per collector	30	l/h
Timespan	87600 (10 years)	hours
Time step	1	hours

5.2   Sensitivity Analysis- Type of soil

In order to investigate the influence of the type of soil in which is the system working, several simulations were launched. The effect of the type of soil can be assessed through the parameters that depend of it: "Thermal soil conductivity", "Thermal capacity of the soil" and "Density of the soil".

In table 5 the complete set of values can be retrieved:

Table 5 Data set for the sensitivity analysis of the property: soil type

SOIL	THERMAL CONDUCTIVITY (W/m)	THERMAL CAPACITY (J/Kg*K)	DENSITY (Kg/m^3)
GRAVEL	0.77	1000	2000
LIMESTONE	1.5	2000	1500
GRANITE	2.7	840	2600
CLAY	1.1	1879	1000
GREEN SOIL	2.7	2600	840

Multilayer soil

The model allows the simulation of complex soils, conformed by several layers of different materials. In fig 13 the vertical view of the simulated soil can be observed.
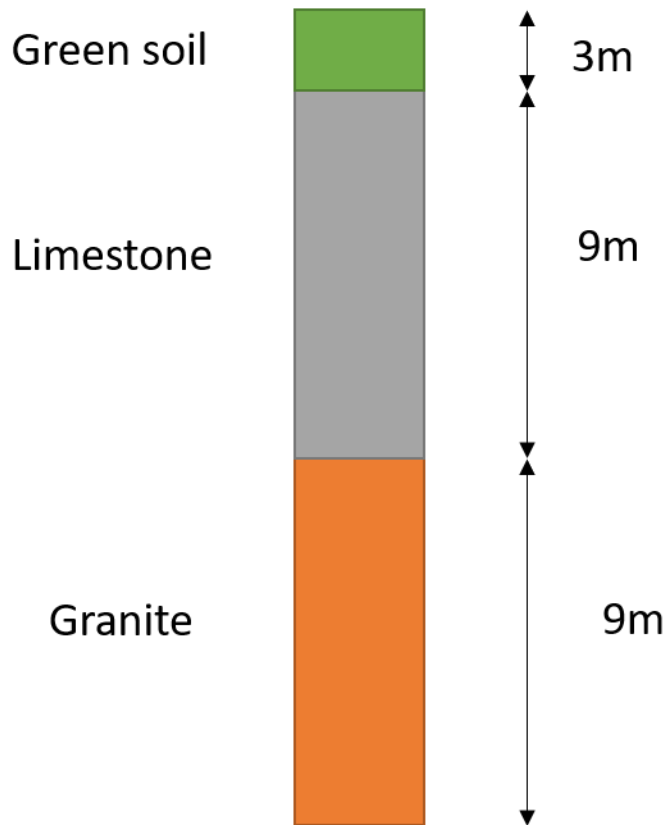

Figure 13 Section of multilayer soil

5.3 Sensitivity Analysis- number of collectors

Number of collectors is also investigated which is closely related with the mass flow in the pipe. This mass flow is related with heat transfer through the convective heat coefficient h. Hence, it gives an idea of the heat that has been transferred to the soil.

In table 6 the number of collectors along with the equivalent mass flow can be seen.

Table 6 Number of collectors and mass flow rate

NUMBER OF COLLECTORS	MASS FLOW RATE (l/h)
1	30
8	240
16	480
32	960
48	1920

5.4 Sensitivity analysis -Mesh size

In order to investigate the effect of the mesh size, different thicknesses of annular regions and vertical layers are studied. The whole set of simulations is summarized in table 7.

Table 7 Mesh sizes and number of elements

THICKNESS OF RADIAL DIVISION (m)	THICKNESS OF VERTICAL LAYER (m)	NUMBER OF RADIAL DIVISIONS	NUMBER OF VERTICAL LAYERS
1	1	8	21
0.2	1	40	21
0.5	0.5	16	42
Exponential distribution with factor $\gamma = 0.2$	1	15	21
Exponential distribution with factor $\gamma = 0.2$	1	30	21

6   Results

In this section all the relevant results for the scenarios in section 5 are presented and discussed.

6.1   Base case

In fig 14 the temporal variation of Temperature at different distances from the borehole wall is presented at depth of 10 m. A lag has been introduced in order to be able to compare the steady state of the soil due to the external temperature with the influence of the borehole.
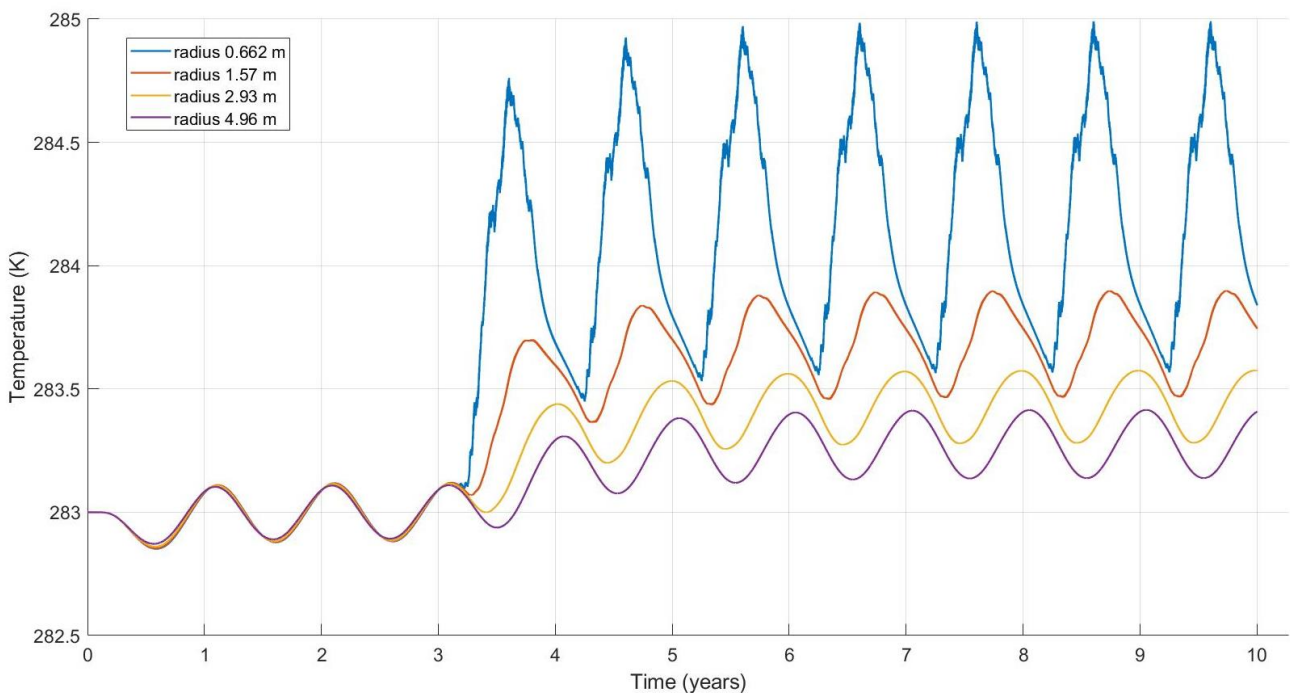

Figure 14 Thermal distribution of the base case for different radial distances at 10 m depth

At the beginning of the simulation some fluctuation due to the surface layer can be observed if fig 14. In the third the BHE starts to work and there is a clear influence.

The interannual effect in the soil at different distances can be observed. Close to the borehole the temperature is higher and it decreases with distance approaching the undisturbed ground temperature of 283K. There is a smoothing of the quick transient process due to the increasingly high capacities of the annular regions. A certain lag can also be observed.

The interannual effect takes place in the third, fourth and fifth years. After that, a steady state regime is reached. The detail of these three years is presented in fig 15.
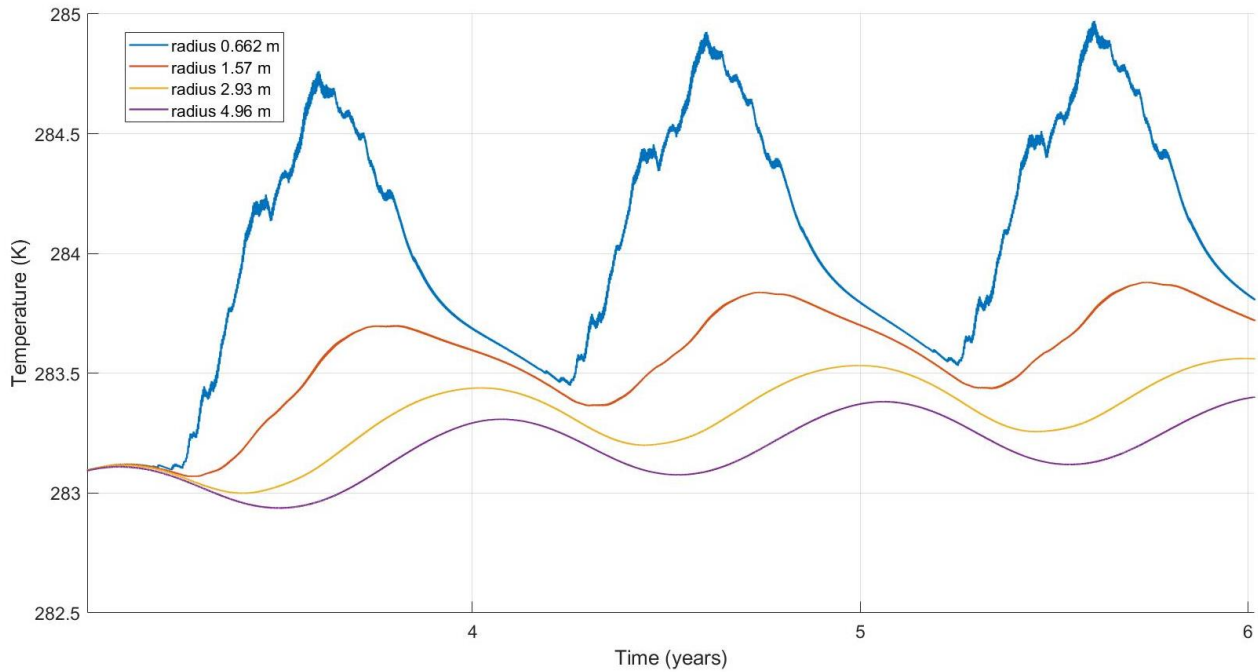
Figure 15 Thermal distribution in the soil. Base-case. Detail of the first three years

As expected during the winter, there is no increment of the soil temperature. However, this situation changes during Spring, reaching a peak in Summer and decreasing in Autumn. Due to the thermal inertia of the soil, this heat remains for a long period in the soil and enables the interannual effect to be seen. The temperature at the end of year 1 is higher than at the beginning.

Data shown is taken at a depth of 10 m, where the effects of the surface temperature are negligible, as shown in fig 16.
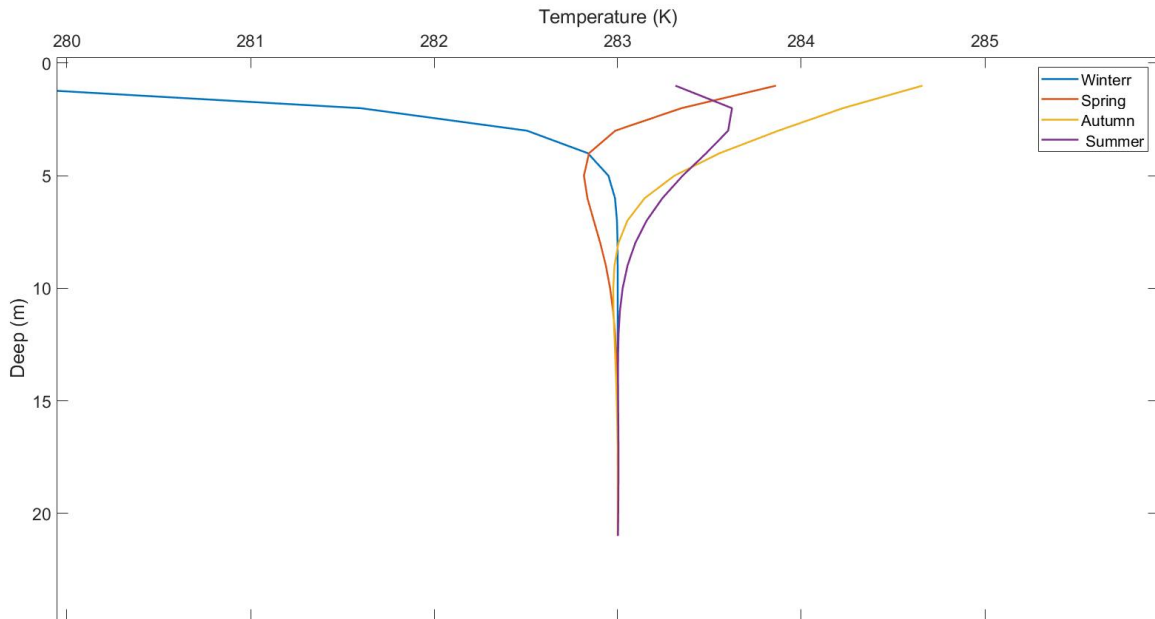
Figure 16 Temperature profile with depth. Base-case

In fig 16 a profile of temperatures with depth can be found. Four series of data that correspond to four different moments of the year are shown each one corresponding to one season. The data shows clearly how the temperature reaches the undisturbed ground temperature at a depth of 15 meters approximately. The series starts at a depth of 1m, where a lot of attenuation has already taken place.

The data belongs to a point far away enough from the borehole not to be influenced by it (8 meters).

It is also interesting to have an idea of the amount of heat that is transferred to the soil from the borehole in order to understand the balance of energy in the soil. Fig 17 shows the annual heat injection.
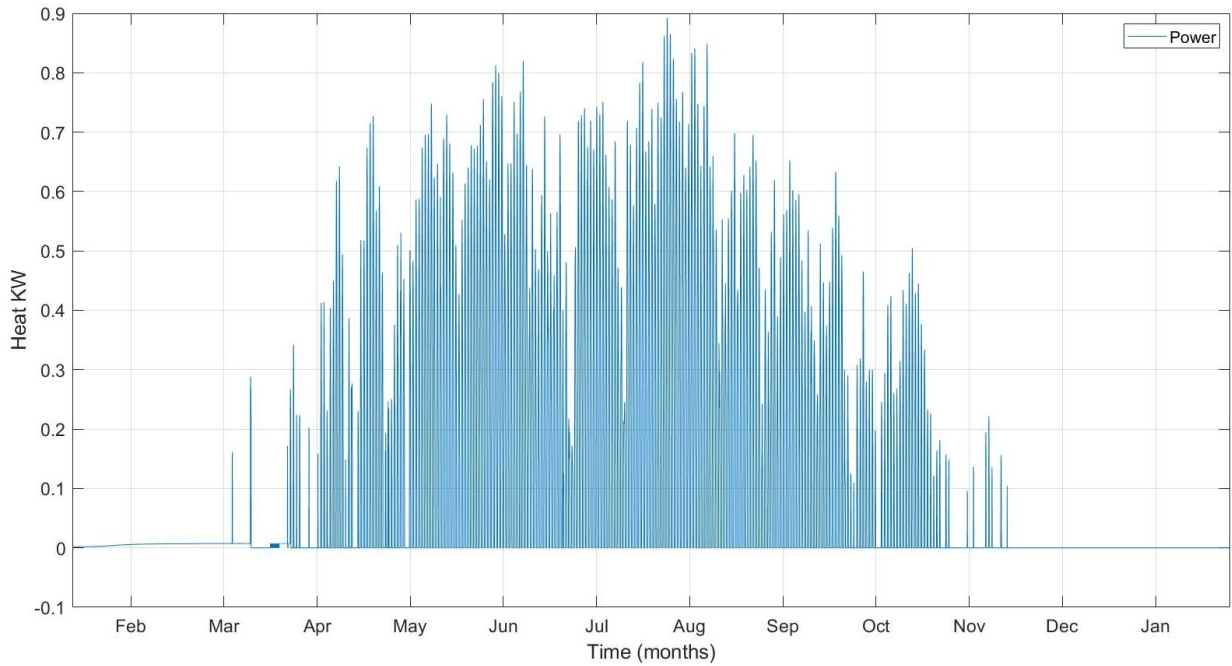
Figure 17 Heat transfer in the borehole during the first year

As can be seen the greater production takes place in the central months of the year with peaks of almost 1 KW. The total amount of heat injected to the soil in a single year is around 3000 MJ.

It is interesting to study how much heat is stored in the soil over the time. This magnitude not only accounts for the heat injection from the BHE, but also the energy exchange between the surrounding soil and the surface. In fig 18 this information is presented for the deeper layers (10 to 21 m).
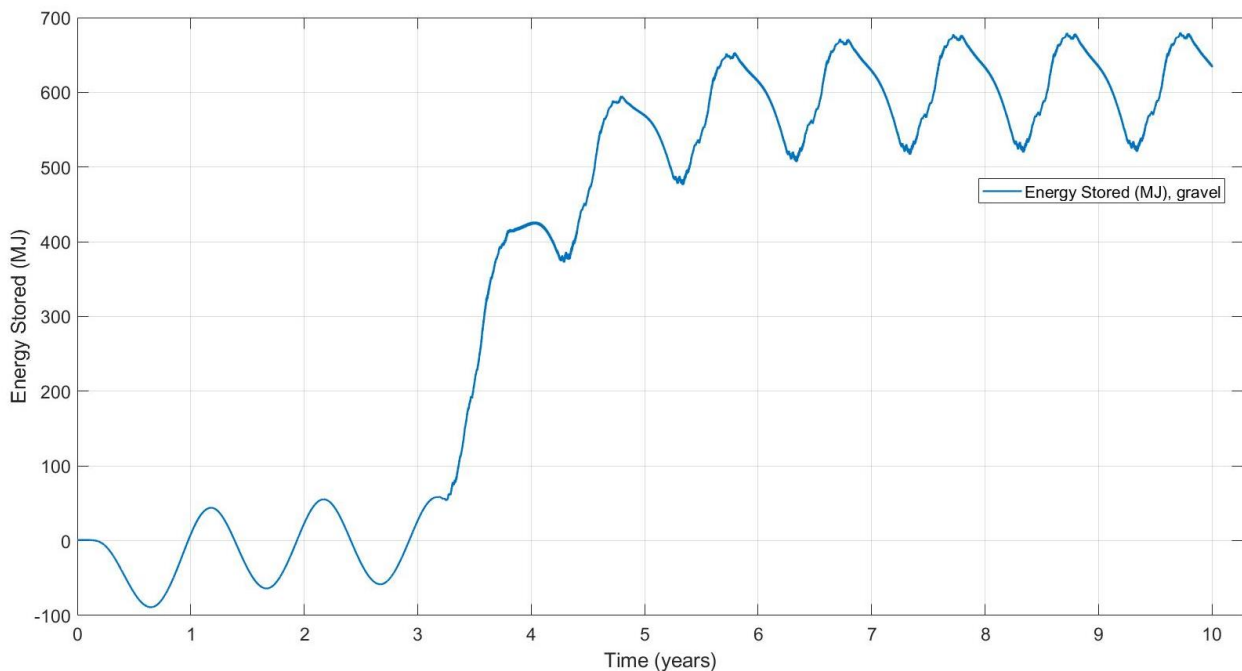

Figure 18 Energy stored in the volume of control from a depth of 10m to 21 m

There is a clear transient effect that is explained as follows: since the energy does not reach the whole control volume at the same time, at the beginning of the simulation just the regions surrounding the borehole increase their temperature and the ones far away remains at Tm. When the heat reaches this far regions, they increase their temperature and they add up to the computation of the heat of the whole control volume according with Eq 37. The total energy stored in the control volume is presented in fig 19.
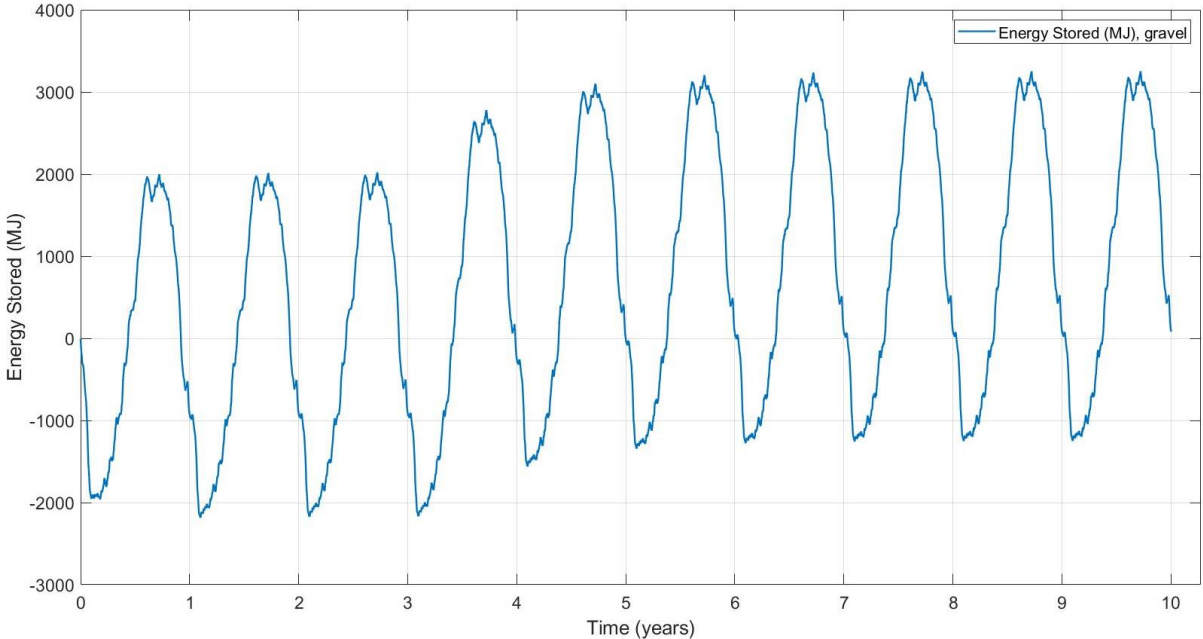

Figure 19 Total amount of energy stored in the control volume

It is clear that there is a strong influence of the temperature of the surface. In fig 18 it has been shown that there is a transient period and a stabilization around 600 MJ. However, in fig 19 the transient effect is less important, and the range of values is huge. The cause for this behaviour is due to the fact that the upper layers of soil have a stronger variation of temperature over the year than the one of the deeper layers as shown in fig 16. Then, the contribution of this regions to the total computation is important compared with inner layers since computation has been carried out by means of Eq 37, where the difference of temperatures is the only parameter that varies.

6.2 Sensitivity analysis

A sensitivity analysis is conducted in order to investigate the effect of the kind of soil surrounding the borehole and the number of collectors attached to it. The dimension of the mesh is also studied.

The thermal behaviour of every kind of soil depends on three variables which appear at a different combination: thermal conductivity, thermal capacity and density.

Another parameter that influences the thermal response is the number of collectors, as it gives the mass flow that is entering the system and therefore, the amount of heat injected. However, as shown in section 2.2 the ratio of heat transfer by convection depends on the Nusselt´s number, which depends at the same time on the Reynold´s number which is a function of speed directly related with the mass flow. Therefore, there is a direct relation between this parameter and the heat transferred to the soil.

Since in section 5 it has been shown that the soil can be considered in steady state when the BHE starts working, the lag has been removed from further figures.

6.2.1 Soil type

In fig 20 the thermal response at a depth of 10 meters is shown for different types of soil The values of thermal conductivity, density and thermal capacity were set following table 5 and section 5.1.
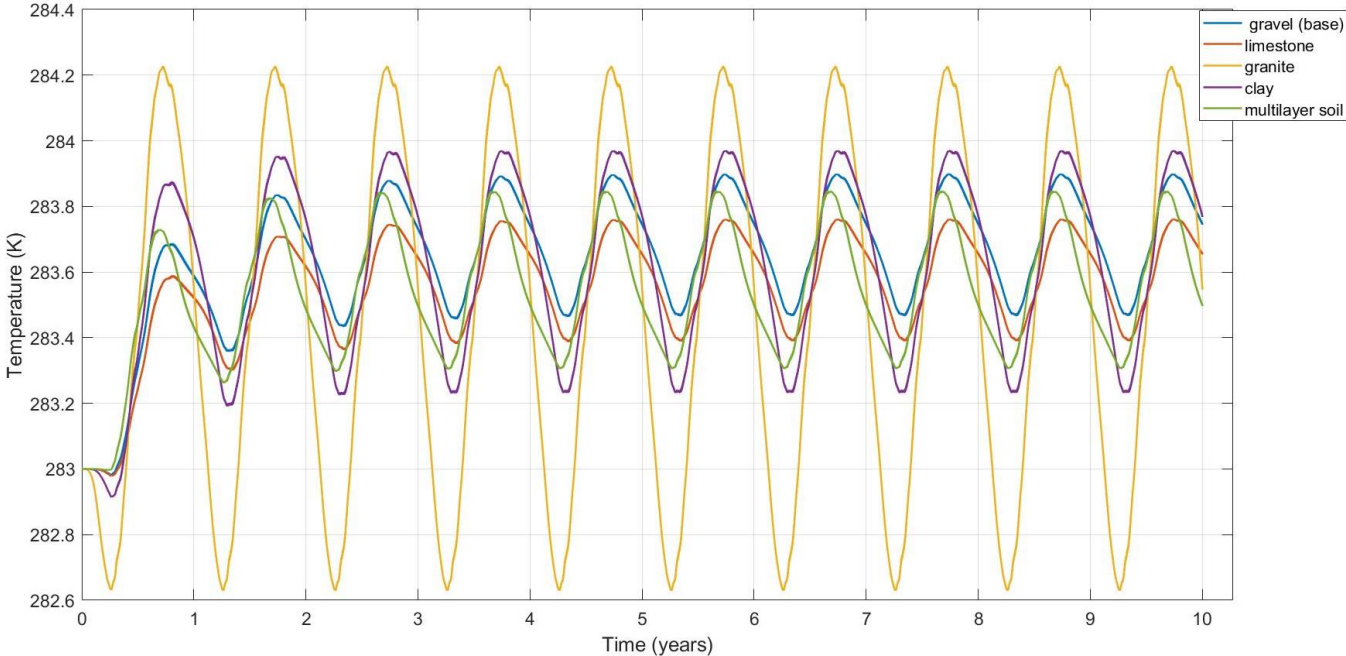

Figure 20 Temporal variation of temperature at 1.58 m from the borehole and 10 depth for different types of soil

As can be seen, there are differences depending of the type of soil chosen. Thermal behaviour of soil depends as explained in section 2.2 on three parameters: Thermal conductivity, density and thermal capacity. The lower the thermal conductivity is, the longer the transient effect and the lower the change in temperature. It is remarkable that the base case and limestone show a very close response although there is a big difference in its thermal conductivity. This could be due to the comparatively higher value of thermal capacity of limestone compared with that of gravel ($2000 \frac{J}{kg*K}$ vs $1000 \frac{J}{kg*K}$). In figure 21 the detail of the first year is presented
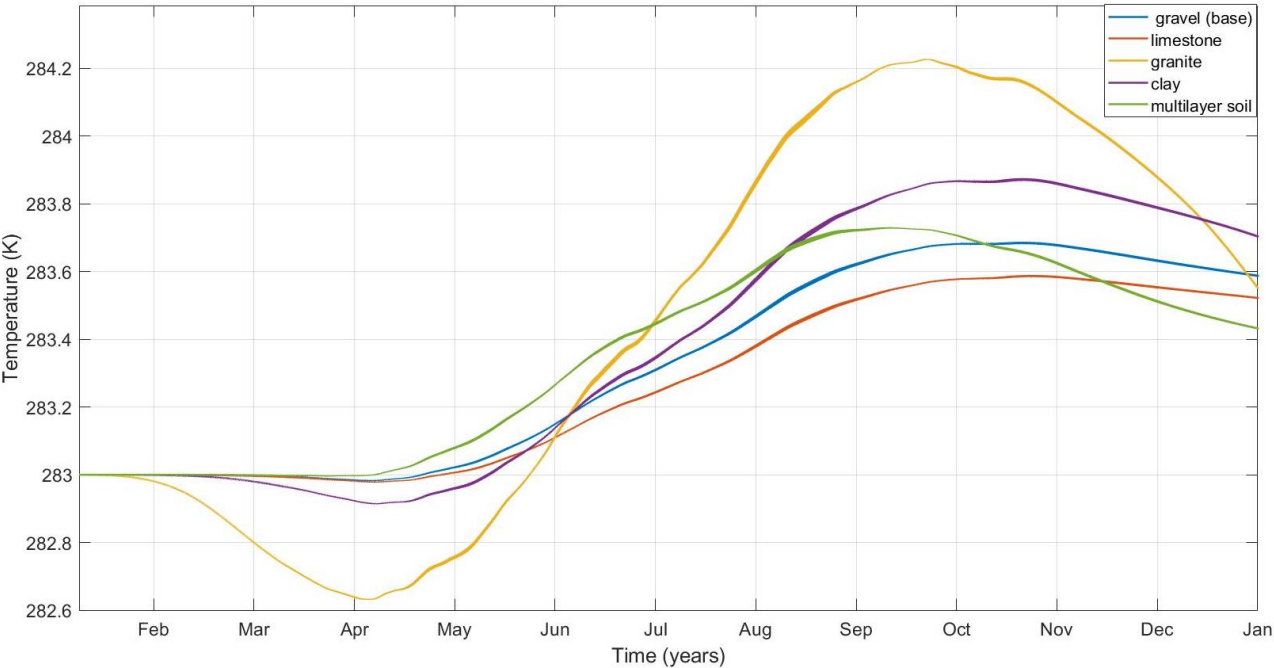

Figure 21 Sensitivity Analysis -Type of soil, Temporal variation of temperature at 1.58 m from the borehole and 10 depth for different types of soil. Detail of the first year

The figure show how the effect starts to be important from April, except for granite, and reaches a peak in October and November. It is noticeable that the peak in the temperature inlet took place in the months of August and July, the lag lasts then for two months. At the end of the first year the increment of soil temperature is between 0.4 and 0.8K.

The case of granite is special, for that it shows a very quick response. This can be due to the relatively small thermal capacity (840J/kgK) that is inherent to this material.

Regarding multilayer soil, at 10 m depth the layer shown is made of limestone, but the evolution of temperature is different that the soil made just of limestone.There is an influence of the other layers, that are conformed by different materials. In fig 22 results at radius 1.58 and different depths are shown for the multilayer case for the first three years.
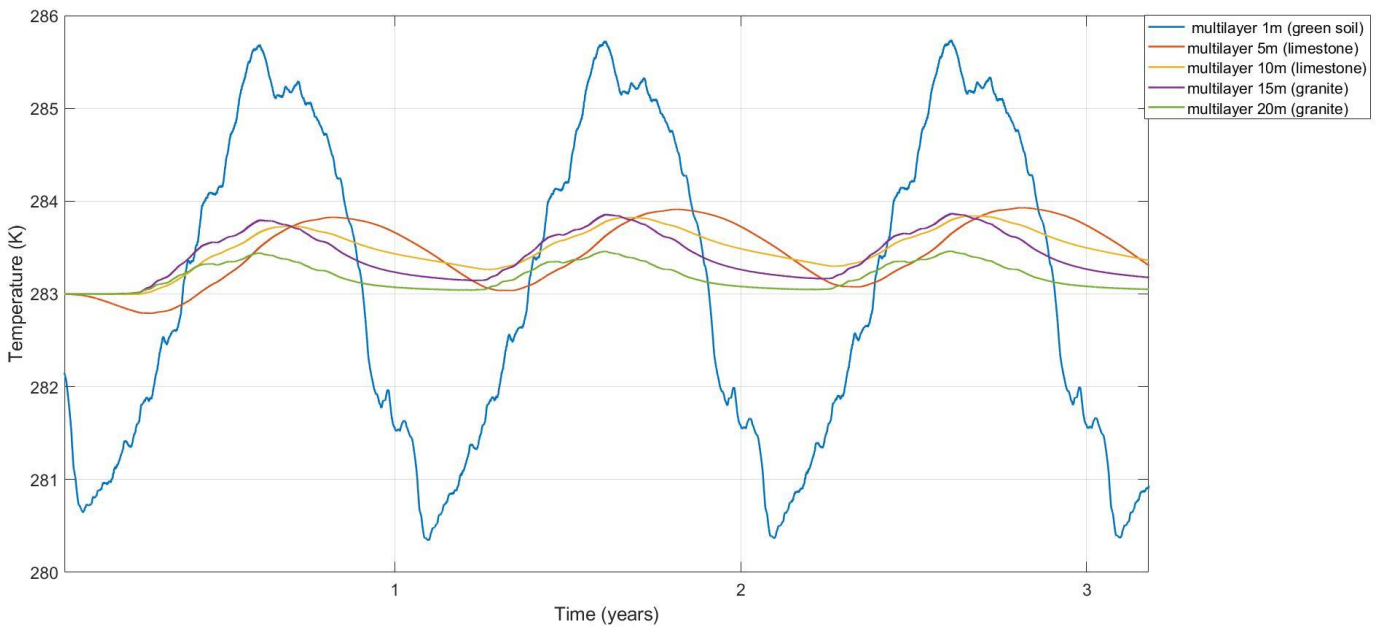
Figure 22 Sensitivity Analysis. Type of soil. Temperature at 1.58m from the borehole and different depths for a multilayer soil.

As can be seen, the influence of $Tsurface$ is big from 1 m to 4 m depth. However, at deeper layers this effect is negligible and different lags can be observed. The change of material is located at 12 m depth. At 10 meters (limestone) the range of temperatures is similar to the one at 15 m(granite). The cooling down of limestone is slower than that of granite.

Regarding energy stored in the control volume, a comparative of the different types of soil has been conducted whose results can be found in fig 23.

In this case just the depths below 10 m have been considered in order to show the removal the influence of the surface temperature.
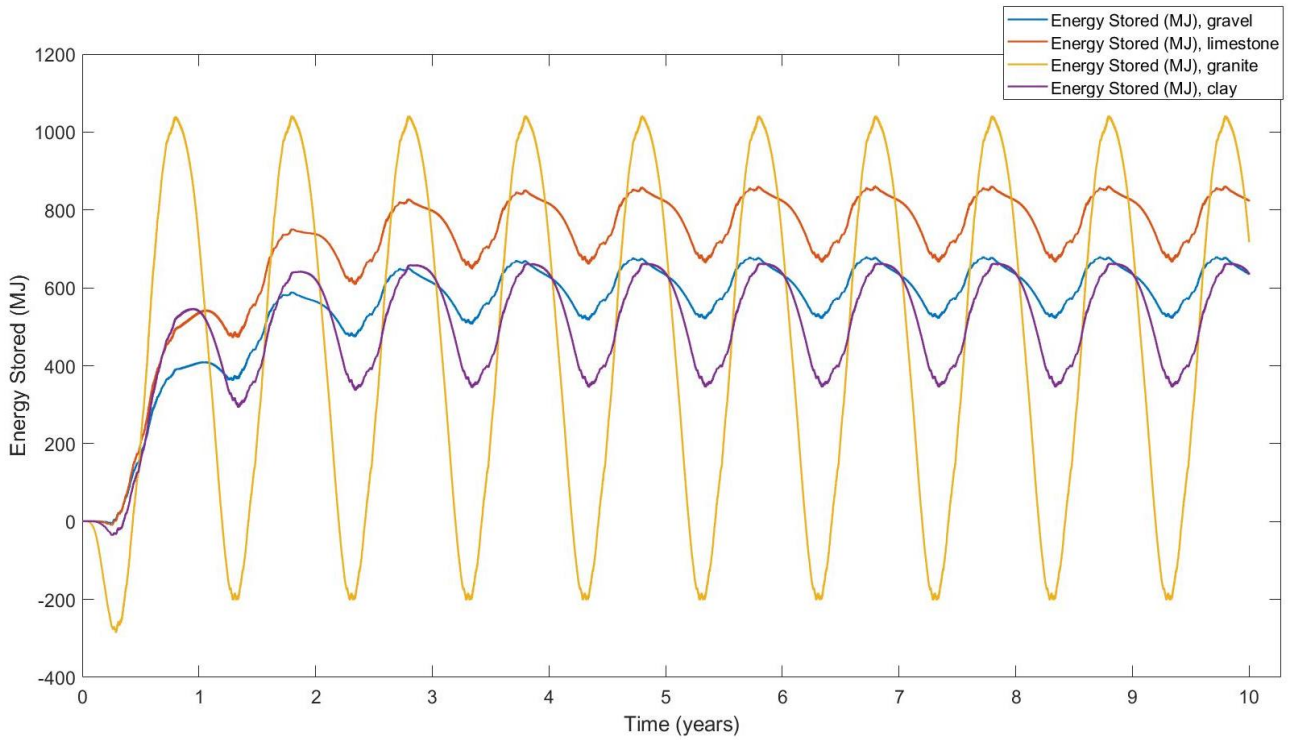
Figure 23 Stored energy in the control volume from a depth of 10 m to 21 m

A transient effect can be seen for the different types of soil considered, except for granite. In the case of granite, there is a big variation due to the small thermal capacity of this material.

6.2.2   Number of collectors

In figure 17 a different analysis was conducted. In this scenario the variable that was modified was the number of collectors, which has been previously discussed to influence the mass flow of the system. In Table 5 the equivalent flow rate for every number of collectors is shown.
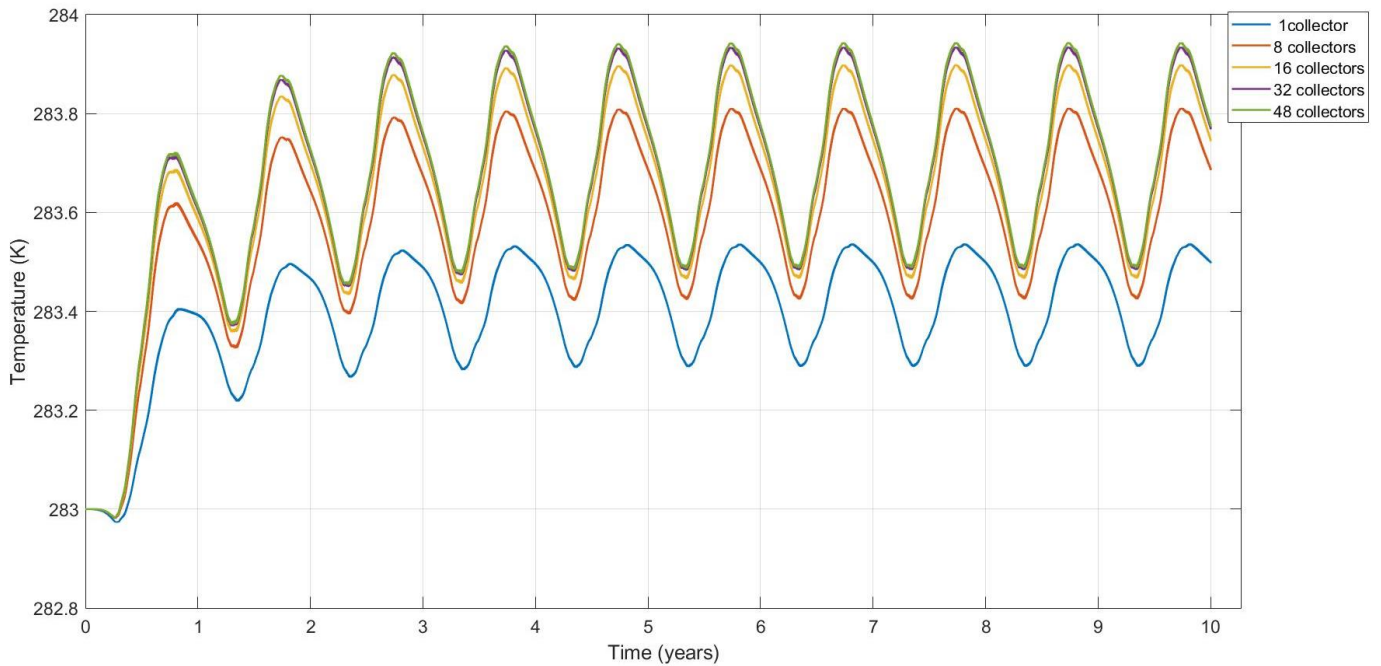

Figure 24 Sensitivity Analysis - Number of collectors

In this figure the data is taken again at 10 m depth and 1.58 m away from borehole center. As can be seen, the effect of this variable is not remarkable. There is a difference in the case of having just one collector supplying the flow rate, but for 16, 32 and 48, the results are nearly the same.

This phenomenon can be explained because of the value of the Rfc which has a non linear behavior. The dependence of Rfc with mass flow rate and the geometry of the pipe has already been presented in section 2.1.3

The value of Rfc is shown In fig 18 for the different values of flow rate that enter the system.
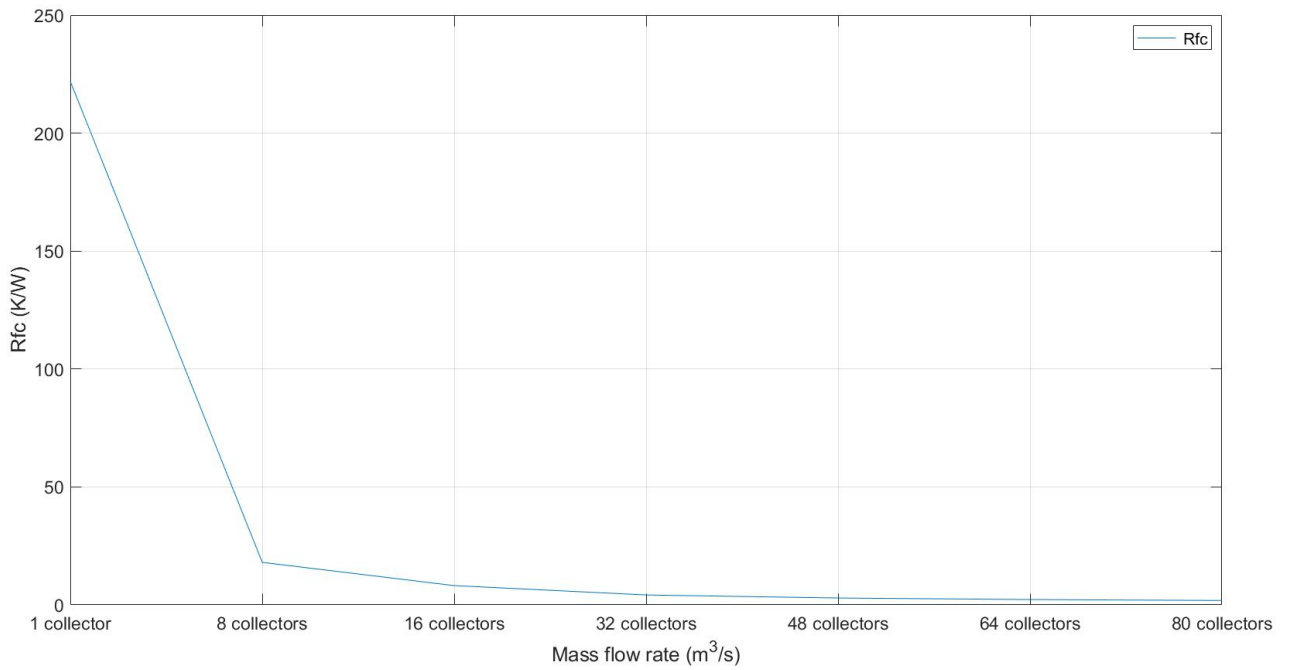
Figure 25 Rfc against mass flow rate

With low resistances, the heat transfer is higher, however since the decrement of Rfc follows a negative exponential behavior, the increment of heat will increase in the same way that Rfc decreases. That explains why there is a big difference between working with 1 collector and 8 collectors, but a small one between having 32 or 48 collectors.

6.2.3 Mesh size

In figure 26 the profile of temperatures in the radial direction is found for a certain moment of the simulation (22 June of the first year at 12 a.m). The values approach with increasing distance to 283K, which is the undisturbed ground temperature.

The shape of the profile shows that the decrement in temperature is greater in the proximities of the borehole from 0 to 2m.
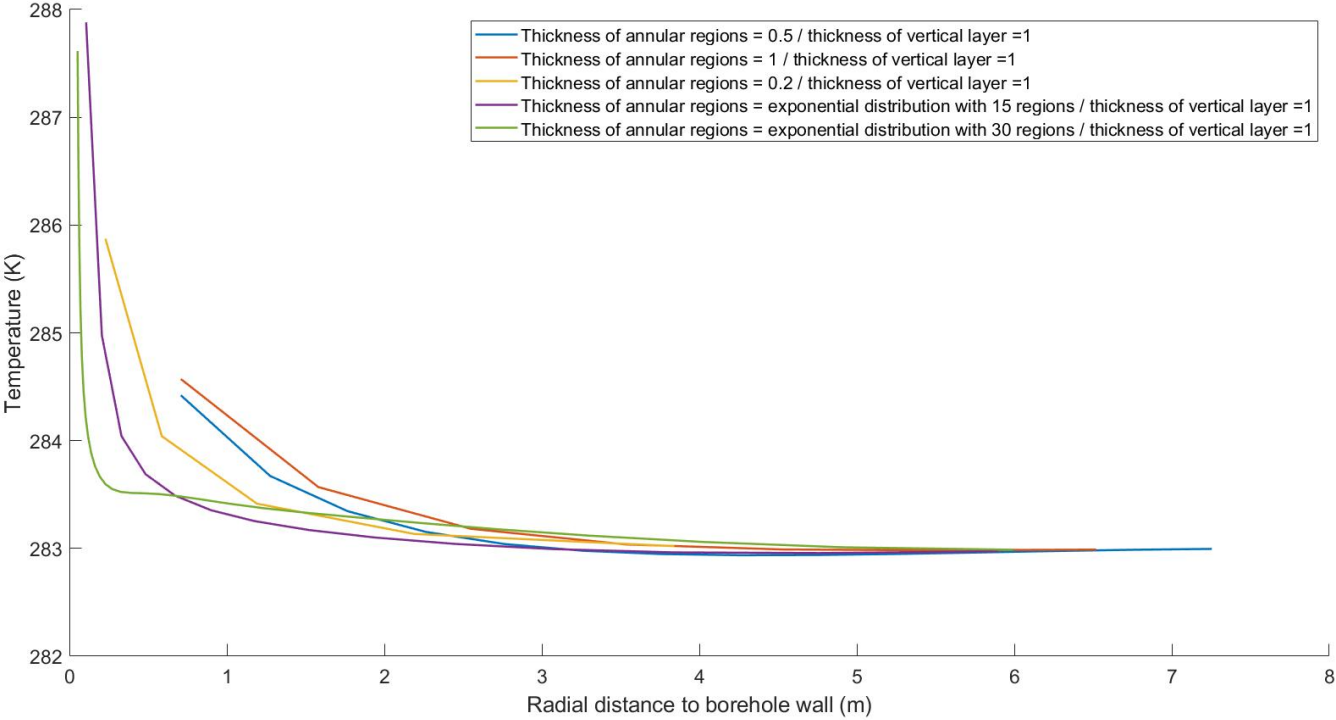

Figure 26 Temperature profile in the radial direction for different combination of mesh dimensions at a time of simulation equal to 4835 h

As found in (Xu , Xiang , & Shuyang , 2017) models with smaller mesh size provide more accurate results, but the time of computation increases exponentially. However, the results may be accurate enough with relatively big mesh size.

It is clear from fig 26 that the differences in the calculation of the base case (red line) are negligible from 3 meters to *rmax*. However, there is big difference when distance ranges from 0 to 3 meters. In figure 25 the temperatures of the radial points with exponential distribution of 15 layers are presented.
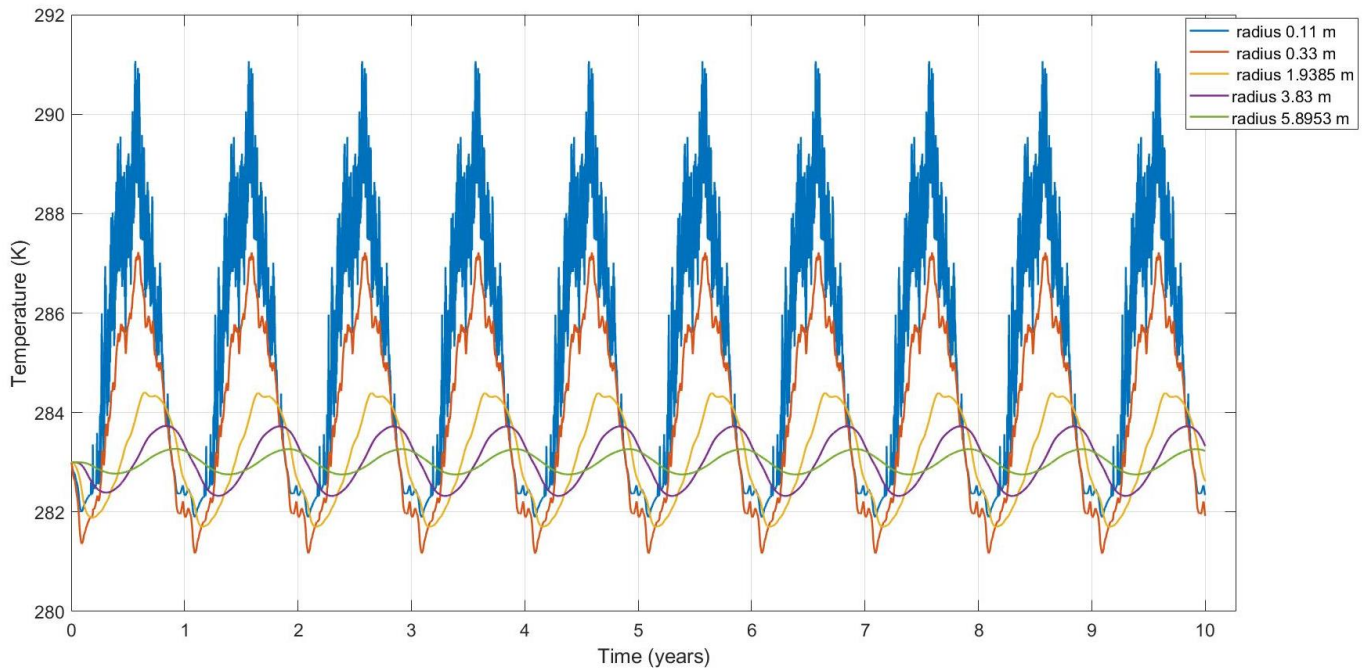
Figure 27 Radial temperature at 10 m depth with exponential mesh distribution of 15 regions and $\gamma = 1.5$

As can be observed, the temperature in the proximities of the borehole wall has a higher temperature. Ideally, at point 0 the temperature of the borehole wall can be found. There is however a difference between the values of the points far away from the borehole predicted with this model and those shown in fig 14.

It is also remarkable the absence of interannual effect. This can be according with (M. Diaz-Aguiló, 2014) a consequence of the choose of the mesh size.

In order to capture fast transients, big order models are required. This high order models allow to capture the slow transients as well but require a big computation time. On the other hand, slow transients require a lesser number of regions because the slow dynamics are predominant, and they just can be seen by means of big capacitances. However, the use of too thick regions can lead to non-physical barriers, and therefore a misrepresentation of the temperature. (M. Diaz-Aguiló, 2014) .

This manifest that the correct selection of the parameter γ of the exponential distribution is of critical importance for the right modelling of the soil.

7   Conclusions

The main goals of the study have been accomplished since the tool that has been developed allows the simulation of the BHE. More importantly, it allows to carry out simulations with different parameters that can be easily edited and that can be related with other Matlab scripts within the HySol project.

Soils with low thermal conductivities present slower transient responses and therefore are more adequate for seasonal heat storage.

It has also been shown that the increment of temperature in the soil with mass flow approaches a steady value with 16 collectors, therefore the addition of more collectors will not lead to a direct increment of stored energy in the soil.

The simulations with different mesh sizes allow to have accurate results with low computational time. With small meshes quick transients are captured, but when these quick transients are mitigated by the effect of thermal inertia, bigger meshes are required. A good selection of the parameters of the exponential distribution is vital to obtain accurate results.

7.1   Limitations and further studies

However, the model has some limitations. First of all, the value of *Tsurface,* although based in the ambient temperature, is arbitrary. This problem is difficult to solve, as it is a value that depends physically on the energy balance in the surface, that accounts for radiation from the sky and from the soil, convection that must include vegetation…

Other limitation is the fact that the mass flow rate is constant or zero. This is not realistic, and the main obstacle is that the matrix A depends on this value. This problem can be solved by a discretization of different values of flow rate and the calculation of the correspondent matrices

Finally, selection of the mesh in this study has been conducted manually. A method that optimizes this selection could be interesting as a study derived from this one.

8 References

Alam, M. &. (2015). *Underground Soil and Thermal Conductivity Materials Based Heat Reduction for Energy Efficient Building in Tropical Environment.* Indoor and Built Environment. 24. 185-200. 10.1177/1420326X13507591.

Al-Chalabi, R. (2013). *Thermal Resistance of U-tube Borehole Heat Exchanger System: Numerical Study.* Manchester: University of Manchester.

Bennet, e. a. (1987). *Multipole Method to Compute the Conductive Heat Transfer to and between Pipes in a Composite Cylinder.* Department of Building Physics, Lund Institute of Technology, Lund, Sweden.

D. Bauer, W. H.-S.-J. (2010). Thermal resistance and capacity models for borehole. *International Journal of energy research.*

Dalla Santa, G. e. (2017). *Laboratory Measurements of Gravel Thermal Conductivity: An Update Methodological Approach.* Padova: European Geosciences Union General Assembly 2017, EGU Division Energy, Resources & Environment, ERE.

De Vries, D. (1963). *Thermal properties of soils. Physics of Plant Environment.* Physics of Plant Environment. North-Holland, Amsterdam, pp. 210-235.

De Vries, D. (2002). *The thermal conductivity of soil. Final project report.* Landbouwhogesch.

Dittus FW, B. L. (1930.). *Heat Transfer in Automobile Radiators of the Tubular Type .* Publications in Engineering 2, p. 443, Univ Calif (Berkeley).

Evans, T. D. (2010). *The increasing potential for ground source heat pumps.* ICIBSE Journal posted April 2010.

Fürtbauer, D. &. (2019). *Investigation of Pipeline Heat Loss to Ground Influenced by Adjacent Pipelines.* ILF Consulting Engineers.

Gu, Y. O. (1998). *Development of an equivalent diameter expression for vertical U-tubes used in ground-coupled heat pumps.* ASHRAE Transactions Vol. 104, pp. 347–355.

Helge Skarphagen, D. B. (2019). *Design Considerations for Borehole Thermal Energy Storage (BTES): A Review with Emphasis on Convective Heat Transfer.* Hindawi Geofluids Volume 2019 26 pages https://doi.org/10.1155/2019/4961781.

Hellström, G. (1991). *Ground Heat Storage: Thermal Analyses of duct storage systems.* Lund, Sweden: Department of mathematical physics. University of Lund.

Incropera, F. P. (2007). *Fundamentals of Heat and Mass Transfer. 6th edition.* Wiley.

Intemann, P. (1982). *Towards Solving The Conflict Between Geothermal Resource Uses.* Master thesis for the Energy Division in Oak Ridge National Laboratory,Tennessee.

Johansen, O. (1977). *Thermal conductivity of soils.* Corps of engineers U.S Army.

Kersten, M. (1949). *Thermal Properties of soils.* University of Minnesota, Institue of Technology. Bulletin nº 12 I.

Kurevija, T., Domagog, V., & Vedrana, K. (2011). Influence of Undisturbed Ground Temperature and Geothermal Gradient on the Sizing of Borehole Heat Exchangers. Linköping: World renewable energy congress Sweden.

M. Diaz-Aguiló, F. d. (2014). *Ladder-Type Soil Model for Dynamic Thermal Rating of Underground Power Cables.* Department of Electrical and Computer Engineering, NYU Polytechnic School of Engineering, New York University, Brooklyn, NY 11201 USA.

M. Díaz-Aguiló, F. d. (2015). *Ladder-Type Soil Model for Dynamic Thermal Rating of Underground Power Cables.* Department of Electrical and Computer Engineering, NYU Polytechnic School of Engineering, New York University, Brooklyn, NY 11201 USA.

Schlünder, E. (1983). *HEDH – Heat exchanger design handbook, vol. 2.* New York: USA: Hemisphere Publishing Corporation.

Sharqawy, M. M. (2009). *Effective pipe-to-borehole thermal resistance for vertical ground heat exchangers.* Geothermics. Vol. 38,pp. 271– 277.

Shonder, J. A. (1999). *Determining Effective Soil Formation Thermal Properties From Field Data Using a Parameter Estimation Technique.* ASHRAE Transactions, 105(1).

Silva, A. J. (1985). *The sensitivity of sediment physical properties to changes in temperature, pressure, and porosity.* Collection colloques et séminaires - Institut français du pétrole. 1986, Num 44, pp 289-309 ; Table ; ref : 2 p.

Silwa, T. &. (2015). *Natural and Artificial Methods for Regeneration of Heat Resources for Borehole Heat Exchangers to Enhance the Sustainability of Underground Thermal Storages: A Review.* Andrew Kusiak. Sustainability 2015, 7(10), 13104-13125; https://doi.org/10.3390/su71013104.

Tarnawski, V. F. (2000). *Modelling approaches to predicting thermal conductivity.* International journal of energy reseatch 24:403-423.

Xu , Z., Xiang , Z., & Shuyang , T. (2017). A revised thermal resistance and capacity model for the ground heat exchanger under freezing soil conditions and thermal performance analysis. *10th International Symposium on Heating, Ventilation and*

Air Conditioning, ISHVAC2017, 19-. Jian: Institute of HVAC Engineering, Tongji University, Shanghai, China 201804.

Zarrella, A., De Carli, M., Tonon, M., & Zecchini, R. (2009). *A computational capacity resistance model (CaRM) for vertical ground-coupled heat exchangers.* Elsevier, Applied Energy 112 (2013) 358–370.